DESIGN CONSIDERATIONS FOR MID-RISE STEEL FRAME STRUCTURES USING WOOD-BASED FLOORING SYSTEMS

by

Tobias Fast

B.A.Sc., The University of British Columbia, 2013

A THESIS SUBMITTED IN PARTIAL FULFILLMENT OF

THE REQUIREMENTS FOR THE DEGREE OF

MASTER OF APPLIED SCIENCE

in

THE FACULTY OF GRADUATE AND POSTDOCTORAL STUDIES

(Civil Engineering)

THE UNIVERSITY OF BRITISH COLUMBIA

(Vancouver)

October 2014

Abstract

This thesis discusses design considerations for mid-rise steel frame structures using wood-based flooring systems. Gravity load design aspects including composite behaviour, structural weight, floor vibration and lateral bracing are considered for joisted and panel floors in steel building structures. The influence of joisted wood-based flooring systems on the seismic response of concentrically braced steel frame buildings is assessed based on linear dynamic analyses and the strength and stiffness demands are compared with capacities provided by the Canadian Wood Design Manual.

Preface

This dissertation is original, unpublished, independent work by the author, Tobias Fast, under the supervision of Dr. Siegfried Stiemer and Dr. Solomon Tesfamariam.

Table of Contents

List of Tables

List of Figures

List of Symbols

a = plan aspect ratio

A = diaphragm area (m^2); chord area (mm^2); cross-sectional area (mm^2)

A_b = bearing area (mm^2)

B_r = steel bearing capacity (MPa)

B_V = shear through thickness rigidity, N/mm

E = elastic modulus (MPa)

$E_{long.}$ = elastic modulus longitudinal to grain (MPa)

$E_{rad.}$ = elastic modulus radial to grain (MPa)

$E_{tan.}$ = elastic modulus tangential to grain (MPa)

f = frequency (Hz)

g = gravitational constant = 9.81m/s^2

G' = steel-concrete composite deck shear flexibility (MPa)F = lateral diaphragm force (kN)

F_i = lateral storey force, storey i (kN)

f_y = yield strength (MPa)

f_c = compressive strength (MPa)

F_{cp} = compressive resistance perpendicular to grain

J_{sp} = species factor (-)

K_B = Length of bearing factor

K_{Zcp} = size factor compression perpendicular to grain

k_d = global diaphragm stiffness, (kN/mm)

k_f = global frame stiffness, (kN/mm)

l = diaphragm length

Q_r = wood bearing capacity (MPa)

r = relative stiffness ratio (diaphragm/frame)

R_D = force modification factor, ductility (-)

R_O = force modification factor, overstrength (-)

u_D = diaphragm deflection (mm)

V_D = diaphragm design shear force (kN)

V_{Di} = diaphragm design shear force for storey i, (kN)

V_{rs} = diaphragm shear capacity (kN)

v = averaged diaphragm shear force (N/mm)

W = diaphragm width (mm)

Φ = performance factor (-)

Δ = deflection (mm)

γ_i = storey overstrength coefficient for storey i (-)

Acknowledgements

I would like to graciously acknowledge the contributions of my advisors, Dr. Siegfried Stiemer and Dr. Solomon Tesfamariam, to the expeditious completion of this thesis. Thank you for the deadlines.

I would like to acknowledge the Steel Structures Education Foundation for their generous financial support of this research throughout my graduate degree, your contributions were entirely appreciated.

I would like to acknowledge the NEWBuildS network for providing a platform upon which to base my research and for the opportunity to contribute to the advancement of innovative wood-based building systems in Canada.

I would like to thank my family for their support, understanding, love and incredible tolerance over the many years of my education. I would like to especially thank my father, the influence behind my structural engineering aspirations.

Finally, I would like to thank Dinah for her always genuine, unfailingly humourous, continual, and ever-appreciated support from start to finish.

CHAPTER 1: **INTRODUCTION**

1.1 Timber Construction in B.C.

British Columbia has a long history of timber infrastructure dating back to early colonization when the capital city of New Westminster was constructed from logs harvested along the Fraser River. Owing to vast amounts of forested land, timber was the predominant building material as provincial towns steadily grew in number and height. However in the early 1900's the demand for taller structures grew and the use of mild steel as a primary building material became increasingly popular, leading to the construction of several buildings over 10-storeys high within the emerging town of Vancouver. These buildings included the Sun Tower, the Hotel Vancouver, and the Dominion Building, all of which remain in use to this day. The end of WWII brought a resurgence of construction back to British Columbia as soldiers returned from Europe and began to reinvest in the built environment of the Lower Mainland. The post-war construction boom featured an increasing amount of concrete buildings, owing to the expensive material costs of steel and timber. Concrete was a cheap alternative which could be used to reach and exceed building heights of the pre-war construction period. The material became so prevalent in the Lower Mainland that Vancouver became colloquially known as a "concrete town."

Though the urban landscape of Greater Vancouver continues to be dominated by steel and concrete structures, a new trend has developed of late which has seen a resurgence in the use of wooden materials. The innovation of wood-based building products and an increasing emphasis on energy-conscious construction have allowed engineers to specify wood use in mid-rise applications making the material competitive with concrete and steel once again. Several changes in government policy in recent years have reflected this renewed interest in building with wood. Both the Wood First Initiative and the increase in allowable building height to 6-storeys for wooden structures have provided incentive to the building industry to increase the implementation of wood products in construction.

1.2 Hybrid Construction

The term "hybrid" refers to a partnership between two objects of separate origins. In structural engineering the term "hybrid" is commonly used to describe an element, system, or building that brings together two separate materials or systems, to optimize specific properties of both and create a product superior to the sum of the parts.

Hybridization in structural engineering can be categorized into several subcomponents: element level, system level, building level. Hybridization at the element level commonly refers to using two or more different materials to form a single element. Hybrid elements, as with hybrid systems, may also be referred to as composite elements or systems. The ideal hybrid material uses the relative strengths of one material to overcome the relative weaknesses of the other material, and vice versa. An exceedingly common hybrid element used world-wide is reinforced concrete. Concrete construction is usually cheap and very easy to work allowing architects certain aesthetic flexibility in producing unique shapes and designs, however the materials low tensile capacity makes it quite brittle in structural applications. Conversely, steel has excellent tensile capacity and good ductility however it is generally more expensive and comes in predetermined shapes and sizes, reducing design flexibility. By placing steel reinforcing bars in the regions of tensile stress in concrete a designer can utilize the best of both materials. System level hybridization describes the incorporation of different elements, also made up of different materials, to increase the efficiency, economy and performance of the system. A common application of system level hybridization is in the use of steel nails in fastening plywood sheathing to sawn lumber framing elements. The steel connectors are cheap, easy to install and provide excellent strength, stiffness and ductility. Steel and wood and commonly used in a variety of hybrid systems allowing wood structures to overcome its limitations in creating larger structures. Building level hybridization is intended to combine the desirable attributes of separate systems to create a structure with enhanced behaviour in gravity and lateral loading. Hybrid buildings often use two systems with each individual system exclusively intended to resist either gravity loading or lateral loading. A common hybrid building example which uses not only separate systems but separate materials for each system is the seen in steel frame – concrete core structures. The steel frame is used for large floor spans and vertical columns which provide open spaces within the building and resist gravity loads while a concrete core may be used to house elevators or staircases while providing lateral restraint to the building.

1.3 Material Mechanical Properties

1.3.1 Wood

Wood is an organic, fibrous plant which when processed into its many different forms possesses differing material properties according to the orientation. This quality is known as anisotropy and implies that designers must incorporate the material in a manner which utilizes its strengths and protects its weaknesses.

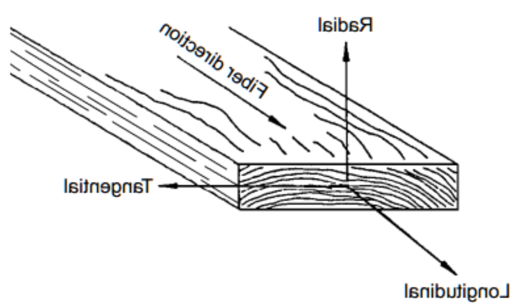

Figure 1: Principal axes of wood (Green, Winandy, & Kretschmann, 1999)

The elastic properties of wood are different for each orthogonal axis shown in Figure 1. The longitudinal axis of wood runs parallel to the fiber direction providing higher stiffness than the radial and tangential directions. The differing properties of wood are commonly referenced by the orientation of the load to the wood grain (longitudinal axis). An axially loaded timber beam-column element has parallel to grain stresses, while the same beam-column element has perpendicular to the grain stresses at bearing locations. The differences between radial and tangential properties are rarely accounted for in strength and stiffness, though they are considered when estimating member shrinkage. A sample of the differences in elastic modulus in the three principal axes are shown in Table 1.

Table 1: Ratio of elastic modulus in the three principal axes (Green, Winandy, & Kretschmann, 1999)

Wood Species	$E_{tan.}/E_{long.}$	$E_{rad.}/E_{long.}$
Douglas Fir	0.050	0.068
Pine (Lodgepole)	0.068	0.102
Hemlock	0.031	0.058
Spruce (Sitka)	0.043	0.078

Design values for compression strength show that an element loaded parallel to the grain is more than twice as strong as when loaded perpendicular to the grain. Imposing large perpendicular to grain stresses on a wood element can cause unanticipated displacements. Issues with vertical displacements in platform-framed wood structures are often noticed at floor-to-wall connections where vertically oriented wall elements (studs) transfer axial load to plates, joists and rimboards, all of which become loaded with perpendicular to grain stresses. Additional displacements are caused by shrinkage displacements in the radial and tangential directions. A comparison of compressive strengths according to orientation is found in Table 2.

Table 2: Compressive strengths of No.1/No.2 sawn lumber (Canadian Wood Council, 2010)

Species Group	Compressive Strength (MPa)	
	Parallel to grain	Perpendicular to grain
Douglas Fir-Larch	14.0	7.0
Hemlock-Fir	14.8	4.6
S-P-F	11.5	5.3
Northern Species	10.4	3.5

Elastic values are a function of wood species, and vary with moisture content and specific gravity. Those species of wood included in the Canadian Wood Design Manual (CSA 086) include douglas fir, larch, hemlock, fir, spruce, pine and northern. In commercially available wood products such as plywood, sawn lumber and glulam, several different species are grouped together since their mechanical properties are similar, for example spruce, pine and fir are grouped together and known as S-P-F, just as douglas fir and larch are grouped and known as D.Fir-L, and hemlock and fir make Hem-Fir. (Canadian Wood Council, 2010) The elastic properties of wood are adversely affected by higher moisture content and hence for a product to be considered dry lumber it must have a moisture content below 19%. (Canadian Wood Council, 2010)

One of the main benefits of wood as a structural material is the comparatively low building weight that can be achieved through use of wood building elements. The range of densities of commercially available wood species varies between 350-550 kg/m^3 (sitka-spruce – douglas-fir). Low material weight translates to benefits in design where reducing building weight reduces foundation material costs as well as in construction where lighter building materials can be transported and moved around site with less restriction and energy. (Green, Winandy, & Kretschmann, 1999)

Commercially available wood products in Canada are also separated into different strength classes according to the National Lumber Grades Authority using two alternate evaluation methods: visually stress-graded (VSG) and machine stress-rated (MSR). Within visually stress-graded elements there are three further strength classes for dimension lumber, beams and stringers, and posts and timbers: Structural Select (SS), No.1 Grade and No.2 Grade (No.1/No.2), and No.3 Grade (No.3), in descending order of strength. Unlike visually stress-graded lumber, under machine stress-rating the elastic modulus of each individual piece of lumber is physically evaluated and given an appropriate rating. MSR lumber is designated only by its grade and not by species, as is done for VSG lumber. The remainder of this report uses values from visually stress-graded lumber. (Canadian Wood Council, 2010)

Wood products utilize these properties in different ways. Apart from a log, the most basic structural wood product is sawn lumber. Sawn lumber pieces are harvested from trees and milled into boards and planks of varying size. More advanced products such as glue-laminated elements, cross-laminated and nail-laminated panels are made up of multiple sawn lumber pieces. Wooden panels use cross-laminated veneer sheets to form a thin, light panel with good in-plane stiffness. Engineered wood products include I-shaped beams utilizing the axial strength of sawn lumber in the flanges connected by a light, flat plywood web.

1.3.2 Steel

Structural (mild) steel is used in many building structure applications. The most common and widely used form of structural steel, mild steel, has a carbon content between 2.1% resulting in a ductile material which can be formed into a variety of different shapes. Unlike wood, steel is an isotropic material and can hence be oriented in any which way the designer prefers with no difference in material strength or stiffness. Building structures use structural steel for vertical columns, spanning elements, lateral bracing and other secondary components.

Unprotected steel elements will corrode when exposed to water. Since corroded steel members can experience large decreases in strength it is it critical to be mindful of designs exposing steel to the elements or areas where standing water can accumulate.

Structural steel has excellent stiffness and strength when compared to standard design values for wood and concrete. Table 3 shows the far superior values for stiffness and strength when compared with two other popular building materials, wood and concrete.

Table 3: Typical design values of engineering properties for steel, wood and concrete

Material	E (MPa)	f_y (MPa)	f_c (MPa)	Density (kg/m^3)
Steel	200 000	400	400	7 850
[1]Wood	11 000	10	[2]142	420
Concrete	25 000	-	30	2 500

[1]D.Fir-L No.1/No.2; CSA 086
[2]Parallel to grain

One drawback of using structural steel members in construction is the relatively high material weight. Mild steel has a density of 7,850 kg/m^3, putting an emphasis on manufacturing economical shapes to reduce the structural weight of a building. High material weight increases loading at all building levels and also creates additional difficulties for transportation of structural elements. However it is also important to consider strength-to-weight ratio (SWR, in units of kPa per kg/m^3) when choosing building materials. 350W steel has a compressive SWR of 45, almost 50% higher than douglas fir (31), and 375% greater than 30 MPa concrete. So although the density of structural steel results in heavy beams and columns, the material becomes very useful when space must be conserved or where long spans are required.

1.4 Research Need

The use of timber and steel at a hybrid element or hybrid system level is not unprecedented. Flitch beams and built-up beams are examples of timber-steel hybrid/composite elements while timber-steel hybrid systems include nailed shearwalls and steel connectors in timber frame construction. Despite the natural union of the two materials in the aforementioned examples, timber-steel hybrids at the building level are far less common. The use of wood floors in steel frame structures is perhaps one of the more feasible hybrid options. Steel frame structures generally use a combination of steel frame element topped with concrete slab to bridge open spans and provide a stiff, strong floor surface. The composite system is commonly achieved using steel beams, open web steel joists, or light gauge steel channels which provide either intermediate support or a continuous pouring surface for the concrete, which may be reinforced for either strength, cracking, or both, depending on the application. Replacing the steel-concrete composite system with either joisted-sheathed flooring or mass timber panels has the potential to provide an alternative system with adequate strength, stiffness and damping properties while decreasing floor and overall building weight leading to reduced member and foundation sizes leading to potential cost savings. Though single-family homes built in the North American stick-frame convention often use steel columns or beams for architectural purposes, creating open spaces or a desired aesthetic, these applications can generally be analysed as timber frame structures rather than a complete steel structure with wooden floors. There exist several built examples of wood-based floors in steel frame construction, as will be discussed in the Case Studies section of this report, however the depth of both analytical and experimental research in this area is relatively shallow.

1.5 Research Objective

This research is focused on feasibility and design considerations of wood-based flooring in steel frame structures. The research has a design-oriented approach following provisions in the Canadian design manuals for wood (CSA 086) and steel (S-16) construction to anticipate potential restrictions, benefits, and efficiency of timber-steel hybrid building systems. Basic structural design aspects unique to timber-steel hybrid systems are explored as well as implications for seismic design in lieu of weight reductions achieved using wood floors. The objectives are achieved through reviews of published research on related work, investigation and commentary of relevant code provisions, and through linear dynamic analysis.

CHAPTER 2: **CASE STUDIES**

2.1 Scotia Place

Scotia Place, a 12-storey residential building located in the central business district of Auckland, was erected in 2000 to become one of the first timber-steel high-rise structures of its kind. By replacing composite concrete floors in a conventional steel braced-frame structure with glue-laminated planks, a tall, lightweight structure with less material costs and a visually appealing floors was created.

The hybrid floor system consists of 1200 mm-wide glulam planks using 35x65 mm lamella, lain over continuous supports where possible to create maximum span lengths of 2900 mm. The slender panels are fastened to steel floor beams by 65 mm long Timberlite® screws drilled up through the underside of the top flange into the wood panel. To prevent sound and vibration transmission between tenant units, 15 mm-high sealers were placed between the flange and panel. Floor panels are only considered to span in one direction to prevent perpendicular to grain stresses. The connection detail is shown in Figure 2.

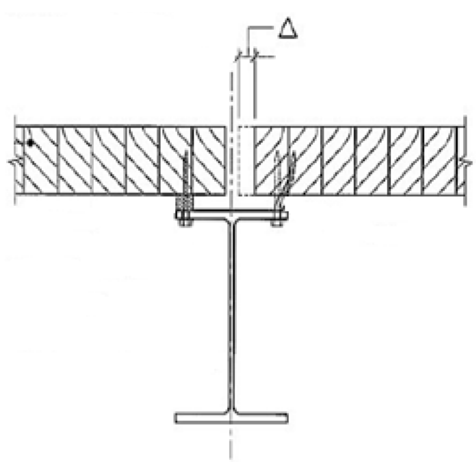

Figure 2: Beam-floor connection detail in Scotia Place (Moore, 2000)

Frame and diaphragm forces for lateral loads resulting from wind and seismic demands were analysed using static and dynamic methods, respectively. Demands from static wind load applied on the widest face of the building governed the design of the concentrically-braced frame. This is not unique for tall structures and is much more commonplace in lightweight buildings, the effect produced in Scotia Place when concrete floors were replaced with wooden panels. Floor accelerations produced by wind loading were checked according to the local code methods which estimated demand based on building density (total weight divided by total volume) and damping. However it was determined that the recommended methods were not suitable for Scotia Place since its building density was so low compared to the data used to establish the code method and since the damping of the novel system was difficult to quantify. In the end it was decided that floor accelerations due to wind loading would not be significant since floor detailing likely provided excellent damping (>5%) and the shape of the building would not produce critical wind loading scenarios.

Linear dynamic analysis of the structure was performed to determine diaphragm forces and accelerations. The methodology of the analysis consisted of modeling the entire structure with rigid diaphragms in ETABS to estimate floor accelerations then applying these accelerations (occurring at the roof) to an individual floor modeled in SAP2000 which would capture diaphragm flexibility. From this analysis designers could calculate maximum floor panel tensile stresses and lateral screw loads. Analysis of deflections of natural frequencies would demonstrate the influence of diaphragm flexibility and any potential dynamic amplification of the whole structure that would not be captured by modeling rigid diaphragms.

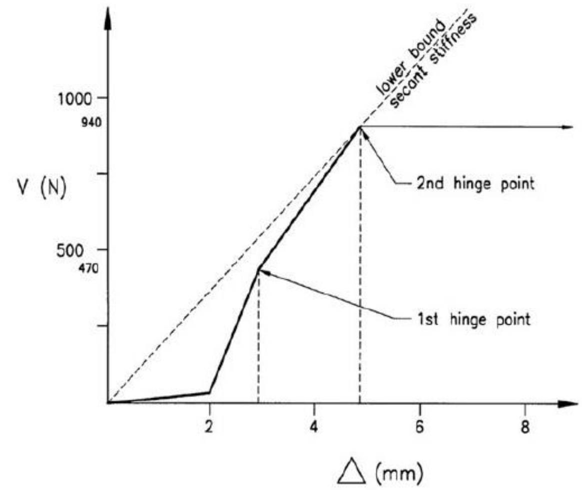

Figure 3: Beam-floor connection response in Scotia Place (Moore, 2000)

The SAP2000 model consisted of a shell element representing the wood panel and a beam element representing the nailed connection. The non-linear load-deflection response and the lower-bound secant stiffness of the floor-beam connection used in the beam element model is shown in Figure 3. The three stages of the load-deflection response resemble initial slip of the nail in the oversized hole drilled into the steel flange, the first plastic hinge forming in the nail and finally the second hinge forming and the connection reaching the yield strength of the nail. It is unclear how this behaviour was quantified by the author.

The results from the flexible floor analysis showed less acceleration, wood stress, and screw load demands then the global analysis performed using rigid diaphragms. It was eventually determined that due to large differences in fundamental period between structure and floor and due to using less actual mass than was incorporated in the model that an analysis using rigid diaphragms was acceptable for design.

The floor vibrations in the hybrid system were estimated with a frequency limit method for the steel beams and static deflection method for the wood floors. Results showed that while the steel beams did not exceed recommended limits, the wood panels did. However it was decided that flooring system was commonly used throughout the country and since connection detailing did not allow for vibration transmission between separate housing units, the floor design would be acceptable. (Moore, 2000)

2.2 Hybrid Timber-Concrete Frame

Finite element modeling of hybrid structures utilizing wooden diaphragms is not unprecedented in published academic works. In 2010 the Chinese research team of Li, He, Guo and Ni presented findings from experimental and analytical work on single-storey, double bay concrete frames fitted with plywood diaphragms. The experimental programme consisted of three diaphragm options, fully sheathed, sheathed with openings, and no diaphragm, within a 2.1-m high, 3.0-m deep, 4.0-m long cast-in-place reinforced concrete frame. Since applied loads were not expected to produce concrete cracking, the same frame could be used for each test. Column end conditions were considered fixed as they were cast into foundation beams, which were, in turn, anchored to the laboratory floor. The wooden diaphragm was made up of 2x6″ joists on 16″ centres framed within perimeter double rim-joists anchored to the concrete frame through ½″ diameter threaded bolts. The floor was sheathed with ½″ OSB plywood nailed every 6″ on the exterior and 12″ on the interior using 2-½″ nails. Hydraulic actuators applied monotonic and cyclic load at three column locations orthogonal to the long direction of the diaphragm.

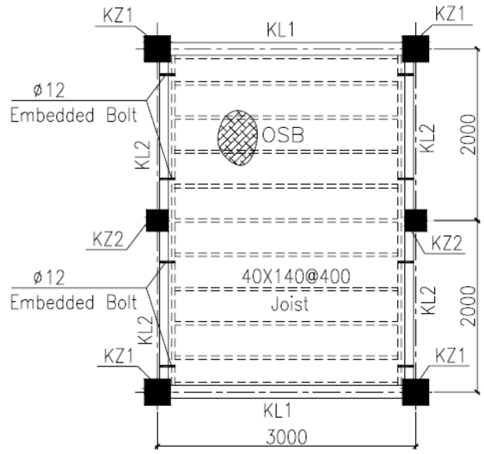

Figure 4: Hybrid concrete-timber test frame (left) and fully sheathed layout (right) (Li, He, Guo, & Ni, 2010)

Testing protocol consisted of monotonic and cyclic loading. Monotonic load was applied on all three diaphragm specimens while cyclic load was only applied to the fully sheathed diaphragm. Monotonic loading was force-controlled with each actuator applying equal load to their respective column. It was observed during the monotonic test on the bare frame that displacements of the middle column were clearly larger than those experienced by the outer columns, indicative of the flexible diaphragm condition. The sheathed floor with openings increased the stiffness of the diaphragm though not to the extent of that seen with the fully sheathed diaphragm.

The cyclic loading phase consisted of two force controlled cycles followed by displacement controlled cycles until the load was reduced to 80% of previous peak load. Test parameter Δ, column-top displacement, was set at 3.5 mm. Cyclic loading was performed on the fully sheathed diaphragm specimen. The testing resulted in cracks forming at the column bases and beam ends at 5Δ displacements and anchor bolt nut slipping at 7Δ. Observations after the testing was completed showed obvious damage to the concrete frame however the wood diaphragm appeared to remain intact. The nut sliding from the rim-joist anchor bolts resulted in asymmetric hysteresis.

The analytical portion of the research by Le, He, Guo, and Ni consisted of four finite element models built in the commercially available structural analysis program SAP2000. A detailed, simplified, flexible and rigid diaphragm models of the experimental set-up were built and compared based on load-deflection behaviour. The detailed diaphragm used frame elements to model lumber joists and concrete beams and columns, shell elements for plywood sheathing, rigid links for the embedded anchor bolts and non-linear springs, based off of physical testing, to represent nail connectors. To reduce the complexity of the detailed model, a simplified version was created that captured the entire in-plane diaphragm behaviour in two diagonal braces. Under the assumption that most non-linearity in real wood structures is located in the shearwalls, the braces were modeled as linear elastic springs. The equivalent stiffness of the springs was determined using a simplified nail deformation behaviour to capture the equivalent diaphragm displacement, which could then be used to calculate the diaphragm elastic stiffness through implementation in the detailed model.

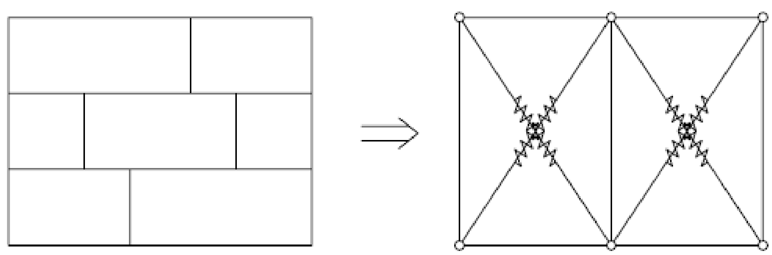

Figure 5: Diaphragm simplification to diagonal springs (Li, He, Guo, & Ni, 2010)

The flexible diaphragm model consisted of the bare concrete frame and the rigid diaphragm model was created by defining all wood elements of the detailed diaphragm as perfectly rigid elements.

Monotonic loading of the four specimens in SAP2000 showed that the simplified diaphragm, when compared to the test results, was adequate in capturing the behaviour of the fully-sheathed diaphragm. A pushover analysis of the models showed that the detailed, simplified, and rigid diaphragms accurately represented the progress of plastic hinging in the actual structure. The diaphragms with meaningful rigidity were able to redistribute loads away from the interior column which was first to experience hinging at its base, meaning the frame with the flexible diaphragm had substantially lower lateral capacity then those with semi to rigid diaphragms. The analysis also demonstrated the appropriateness of using an elastic diaphragm in analysis since the non-linearity of hybrid frames with wooden diaphragms is mostly confined to the vertical lateral load resisting elements. In addition to these findings the researchers concluded that wooden diaphragms more closely mimic the behaviour of rigid diaphragms than flexible ones.

2.3 Hybrid Timber-Steel Frame

In 2012 researchers Ma and He published results from their experimental work investigating the load transfer capabilities of timber diaphragms in timber-steel hybrid structures. Five tests were performed on a 3.0-m x 6.0-m long, 2.8-m high steel frame fitted with a blocked wooden floor testing four different configurations: bare steel frame, two joisted floors with varying nailing schedule, one joisted floor with infilled wooden shear walls. The steel frame was made up of Chinese I-shapes featuring welded and bolted connections infilled with 2″x6″ joists on 12″ centres complete with 5/8″ OSB ply and 3″ nails spaced at 3″ and 6″ on the perimeter and 6″ and 12″ in the interior. Double 2″x6″ pieces were used as intermediate blocking. Loads were applied at each column top with the middle column experiencing twice the load of the individual outer columns.

Figure 6: Hybrid steel frame timber diaphragm experimental tests (Ma & He, 2012)

Four of the five tests were performed monotonically on the bare frame, two diaphragm specimens, and the diaphragm plus wood shear wall specimen. The purpose of the monotonic loading was to investigate the diaphragms influence on lateral distribution of forces in the elastic range of the steel frame. For this reason the same steel frame was utilized for all tests. The bare frame test demonstrated the inability of the link steel beams to transfer load from the middle column to outer columns, meaning the bare case is to be considered flexible. Inclusion of the wooden diaphragms significantly increased the load distribution where each outer column experienced up to 90% of the force in the interior column. The addition of infilled wood shear walls reduced the forces in the outer columns to 75% that of the interior column, due to the reduction in diaphragm to wall stiffness ratio.

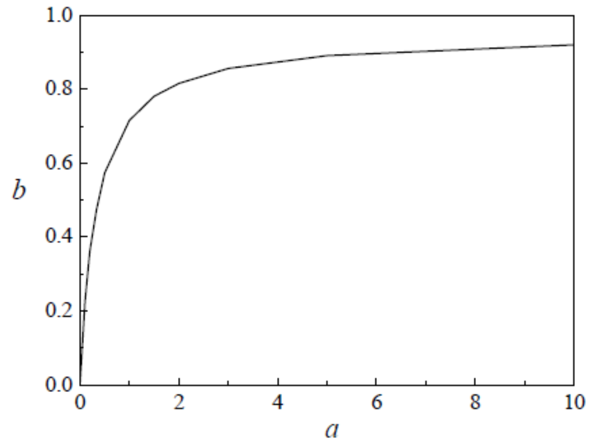

Figure 7: Relationship between lateral load transfer (b) and relative diaphragm to SFRS stiffness (a) (Ma & He, 2012)

Figure 7 provides an excellent summary of the relationship between lateral force distribution to the seismic force resisting system (SFRS) and relative stiffness of diaphragms and SFRS. The vertical axis is the lateral force transfer capability, *b*, where a value equal to unity represents a rigid diaphragm and the null value represents a flexible diaphragm. The horizontal axis describes the ratio of in-plane diaphragm stiffness to lateral stiffness of columns and walls, where larger values of *a* represent a rigid diaphragm scenario. Large increases in lateral force transfer occur at relative stiffness ratios between 0-3, increases in *a* beyond 3 have quickly diminishing impact on the diaphragm force transfer behaviour. Based on the evidence in Figure 7 the authors estimated that for any diaphragms with *a* values greater than 3 a rigid diaphragm assumption would be valid. Little damage was observed in the diaphragm during the monotonic tests indicating that the assumption of diaphragms behaving elastically during the elastic loading phase of the frame is also valid.

Cyclic loading was performed on the diaphragm and infill shearwall specimen to determine the hysteretic behaviour of the hybrid structure as well as to investigate the performance of the diaphragms during inelastic phase of the SFRS. Cyclic tests resulted in nail deformations between sheathing and studs, as well as weld fractures at beam-column joints. Results showed symmetrical, wide hysteresis with indicating good ductility and energy dissipation from the hybrid shearwall system. Despite the damage to the SFRS the wood diaphragm remained intact with minimal damage. The hysteresis for the outer columns was nearly identical to the interior columns, indicating the wood diaphragm adequately distributed lateral forces throughout the inelastic portion of the frame, while remaining undamaged and elastic itself. This result led to the validation of using linear springs to represent the diaphragm in subsequent finite element modeling performed by Ma et al.

CHAPTER 3: **FLOOR PERFORMANCE**

3.1 Introduction to Wood-Based Floors

3.1.1 Floor Spanning Elements

The support of flooring areas in wooden construction can be achieved through either individual joists or by panel segments. There exist many wood-based joists and panels suitable for an array of applications and demands. Joisted construction is exceedingly popular in low and mid-rise North American residential construction, involves individual floor joists spaced out roughly 1′-2′ apart in parallel sequence to produce a light, stiff floor with the added benefit of providing housing for wiring, ventilation and insulation. Panel flooring, widely used in Europe and relatively new to North America, can create construction savings and quality control through pre-fabrication and quick on-site installation. Difficulties with panel flooring include accommodating electrical/mechanical equipment as well connection design and installation. The implementation of either method is largely dependent on project specifics such as aesthetics, dimensions, availability, skilled labour, and cost. Floor design in wood construction is often governed by serviceability criteria, stiffness and sound transmission, rather than strength requirements.

A wide variety of wood-based products can be used in joisted floors. Sawn lumber requires the least amount of processing between the raw and final product and hence are the cheapest and most readily available joist option. In North America most sawn lumber joists are available in 2″ nominal widths and 4″, 6″, 8″, 10″, or 12″ nominal depths and are so prevalent that many construction practices are based off of accommodating these dimensions. Owing to the minimal production requirements, sawn lumber has the lowest engineering properties among joist options (Table 4). An alternative, engineered joists (EJ) are light-weight composite timber sections designed for structural efficiency. A prefabricated element, the engineered joist utilizes the stable I-shape to produce an element stiff in bending capable of long spans. Top and bottom flanges are made of structural composite or sawn lumber pieces connected by a plywood web. Engineered joists provide a superior product in terms of strength and stiffness (Table 4) compared to sawn lumber, however installation is somewhat more difficult as a result of the I-shape when it comes to hanger connections and blocking. EJ are also more expensive than sawn lumber joists. Glue-laminated (glulam) and structural composite lumber (SCL) elements are alternative floor joist options capable of producing long spans and aesthetic appeal. Glulam and SCL are engineered products with larger available dimensions than sawn lumber created with glued laminations of wooden strands, veneers, or sawn lumber to produce a solid rectangular cross-section with excellent engineering properties (Table 4).

Several methods/products are used for creating wooden panel floors. Cross-laminated timber (CLT) panels are made up of perpendicular glue-laminated layers, with each layer consisting repetitive sawn lumber pieces laid flat. CLT panels can be 3-9 layers deep (~310 mm) with maximum dimensions roughly 3 m x 12 m and capable of producing a visually striking floor. The downside to CLT lies in several structural difficulties. Being a relatively new product, methods of analysis for CLT strength and stiffness vary across the research and industry communities. Panel flooring can also be achieved using nail or glue-laminated sawn lumber pieces fastened to each other along the wide face. Whereas joisted floors from sawn lumber or glulam joists use deeper sections spaced 1′-2′ apart, employing the same materials in panel construction smaller section sizes can be used creating a shallow floor depth with equal or improved strength and stiffness properties. Unlike CLT and glulam panels which use glue to fasten laminations, nail-laminated panels (nail-lam) can be manufactured without sophisticated machinery, and can be done so quickly and economically.

Table 4: Engineering properties of floor spanning elements

Type of Flooring	Elastic Modulus (MPa)	Bending Strength (MPa)	Tension Parallel (MPa)	Compr. Parallel (MPa)	Long. Shear (MPa)	Density (kg/m^3)
Joisted Flooring						
Sawn Lumber[1]	9500	11.8	5.5	11.5	1.5	420
Timber	12000	15.8	7.0	11.0	1.5	420
TJI[2]	-	29.7	-	-	5.1	6.7[2]
LVL[2]	13790	28.5	19.8	27.6	3.7	500
LSL[2]	10687	28.8	13.6	22.6	4.0	500
PSL[2]	15168	35.8	25.9	31.9	3.7	500
Glulam[3]	12800	30.6	20.4	30.2	2.0	490
Panel Flooring						
Nail-laminated	9500	11.8	5.5	11.5	1.5	420
Glulam[3]	11000	10.0	5.8	14.0	1.9	490
CLT-1[4]	9500	11.8	5.5	11.5	1.5	420
CLT-2[5]	11700	28.2	15.4	19.3	1.5	420

[1]SPF No.1/No.2; (Green, Winandy, & Kretschmann, 1999)

[2] (Weyerhaeuser, 2010); kg/m

[3] (Canadian Wood Council, 2010)D.Fir-L 24f-EX

[4] (StructurLam, 2012)

[5] (Nordic Wood Structures, 2014)

3.1.2 *Timber-Steel Connections*

Connection detailing in hybrid timber-steel applications is important from both design and construction standpoints. In homogenous buildings where one material is used for all major structural elements (frames, walls), connection detailing is simplified and mostly repetitive. Material properties (strength and thermal related) influence connection design in terms of required bearing, edge and end spacing, connector diameter and allowances for thermal expansion and contraction, hence connecting elements of dissimilar material can increase design complexity. Practical implications also arise in hybrid connections. A flat, continuous flooring surface can be difficult to achieve between joist and beam leading to strict construction tolerances.

Floor-beam connectors are intended to transfer forces and, where required, provide frame stiffness. In steel construction, connections are bolted and/or welded for transfer of shear, bending, and occasionally axial and torsional forces. In wood joist construction a combination of nails and light gauge metal hangers provide transfer of shear forces only, while heavy timber floors (glulam and SCL beams, timber panels) can be detailed to provide some moment resistance through metal brackets, screws and dowels. Floor-beam connections may provide rotational restraint for reducing floor deflection and vibrations, though due to the flexible nature of most light gauge connectors it can be difficult to develop end fixity.

Connections in timber-steel hybrid applications can be done in similar fashion to all-wood construction. Steel connectors such as nails, screws, brackets and hangers are the most common method of joining wood elements and can be used in hybrid construction as well. As with any building structure, connection detailing comprises a significant part of a project and must not only be designed to resist the applied loads, but also be easy to assemble and install while provide a clean, aesthetic look where desired. This section discusses some of the more common wood joist - steel beam and wood panel – steel beam connections found in timber-steel hybrid structures.

3.1.2.1 Joisted Floors: Detailing and Design & Code Provisions

Joisted floors framed within a steel perimeter frame can be constructed in a similar manner to floors in all-wood construction. Typical lumber or engineered joist floors are spaced 250-600 mm apart between perimeter ledgers or intermediate beams and headers using a variety of different fasteners. Most wood-frame residential houses with sawn lumber or engineered joists are hung from ledgers or beams using light-gauge metal brackets, proprietary products known as joist hangers, with punched holes to allow nails to be driven through connecting hanger to wood joist. Joist hangers transfer shear forces from through bearing as well as nail and bracket shear. These metal brackets are widely popular in lightweight wood construction since they are cheap, easy to install, available for any size and application, and have well established performance and design methods. Light-gauge hangers can either be face-mounted or hung from the top flange.

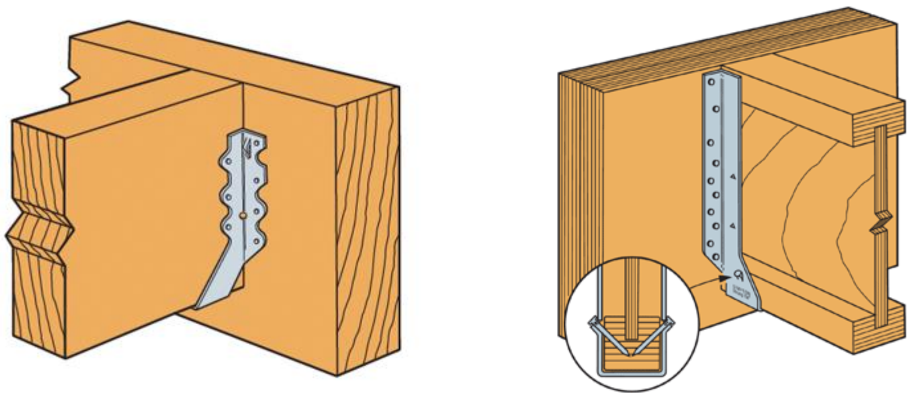

Figure 8: Typical face-mounted joist hangers for sawn lumber and engineered joists (Simpson Strong-Tie®)

Face-mounted hangers provide a bearing seat in which the floor joist rests and a nailing edge to fasten to both the joist and perimeter ledger, as seen in Figure 8. Face-mounted hangers can be used in timber-steel floors by fastening a wooden ledger to the web of the steel section and connecting the joists to this wooden ledger just as one would in all-wood construction. Rows of staggered bolts can be used to fasten the wooden ledger to steel web. This system is quick to assemble on-site and does not require significant preparation aside from drilling holes through the web of the steel flange for the bolted ledger. Once the ledger is in place hangers can be easily fastened and joists are quickly dropped in and nailed in place. This system can be used for sawn lumber, engineered joists, structural composite lumber beams and glue-laminated beams. An example of the system using engineered joists can be seen in Figure 9 and Figure 10.

Figure 9: Examples of engineered joist (top) and sawn lumber (bottom) joist - beam connections using joist hangers and bolted ledgers (studio-tm.com/constructionblog/)

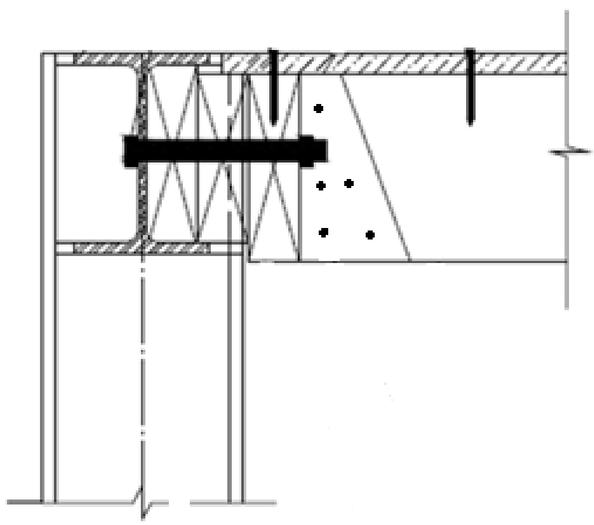

Figure 10: Hybrid steel frame – timber joist picture (top) and connection detail (bottom) (Lam & al., 2013)

In lieu of face-mounted hangers fastened to a wood ledger, joist hangers can be mounted to the top flange of the steel beam directly using a weld or through a nailer board. This system has similar preparation to face-mounted hangers since they must either be welded to the beam or a wooden nailer board must be bolted to the top flange. Use of a wooden nailer board increases the depth of the floor which may be undesirable, though it does have the added benefit of providing a nailing surface for plywood sheathing. Top flange mounted hangers can also accommodate sawn lumber, engineered joists, and structural composite and glulam beams. Images of top flange mounted hangers can be seen in Figure 11 and an application with engineered metal web joists can be seen in Figure 12.

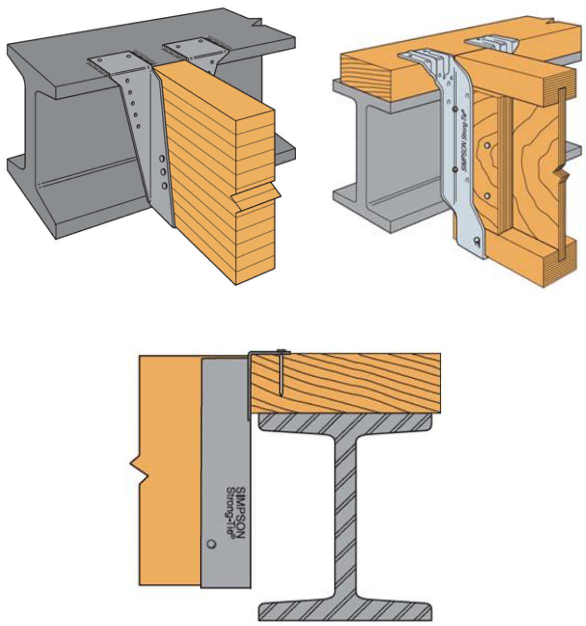

Figure 11: Top flange hanger options for with and without nailer boards (Simpson Strong-Tie®)

Figure 12: Top flange hangers for engineering metal web joists (Apex Timber Engineering)

Larger members such as glulam or structural composite lumber beams can also be face-mounted through knife-plate connections. Knife-plates are welded to steel beam webs and are placed inside a precut slotted hole in the end grain of the wooden beam and bolts are passed through, tying the connection together. Bearing plates can also be used to reduce perpendicular to grain stresses. Knife-plate connections can be used where moment resistance or increased end fixity is required. They also provide aesthetic appeal for exposed applications. Some example details are shown in Figure 13 and an application can be seen in Figure 14.

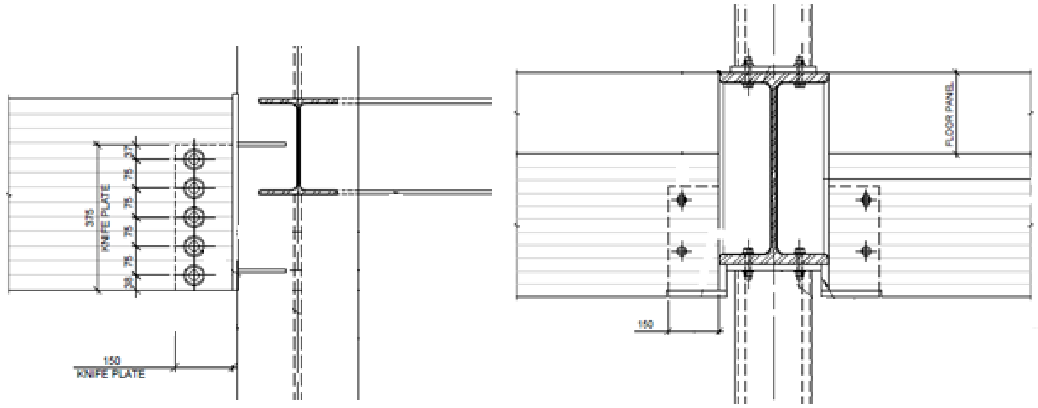

Figure 13: Knife-plate connectors for glulam-steel connections with (top) and without (bottom) bearing plates (Fast+Epp Structural Engineers)

Figure 14: Timber-steel knife-plate and bearing plate connection (studio-tm.com/constructionblog/)

Where continuous spans are desired, joisted floors can simply run over top of intermediate steel beam supports as seen in Figure 15. It may be beneficial to provide a top flange nailer board similar to those in top flange mounted hangers to provide a nailing surface for connecting each joist to the steel beam.

Figure 15: Continuous joisted floors over intermediate steel beams (srt251ckp.blogspot.ca/ & studio-tm.com/constructionblog/)

The design and detailing of joist-beam connections in timber-steel hybrid construction is quite simple when using joist hangers. The only issues to be considered are joist hanger selection and ledger design. The hanger modes of failure and capacities have been calculated by producers and are catalogued in accompanying load tables leaving the designer only the task of determining the demand and selecting the appropriate hanger. In determining the connection demand, CSA 086 stipulates that for proprietary products the calculated demand mustn't exceed 60% of the stated product capacity. Additionally, CAS 086 requires that diaphragm-frame connections be able to resist 3 kN per lineal metre of lateral load. The design of web-fastened ledgers is somewhat more involved, though the process is well covered in CSA 086. Since the ledger is fastened intermittently along its entire length, bending and deflection are of little concern. Perpendicular to grain stresses at bolt locations will govern bolting pattern and size, with reliance on bearing from the bottom steel flange being unacceptable due to possible shrinkage and loss of bearing surface. Designers may choose to place sill gasket between ledger and steel web to prevent moisture contact between the members.

Connections of glulam and SCL elements to steel frames using knife-plate, bearing plate, and other steel connectors are well covered in CSA 086. These connections may be more difficult from a practical standpoint, where providing both a constructible and robust connection without incurring significant connection fabrication costs can be challenging. These connections are also subject to the diaphragm shear transfer requirement of 3-kN per lineal metre.

3.1.2.2 Panel Floors – Detailing and Design & Code Provisions

Timber panel floors in all wood construction are achieved through a series of metal fasteners including many types of screws, nails, dowels, anchors, brackets and straps. Wood panel floors may be rested on top of walls (platform construction) and held in place using vertical or diagonally oriented fasteners, or the panels may be attached to the inside wall face where screws and dowels may be used in conjunction with brackets and bearing plates. Common connection issues faced in all wood construction using timber panels include embedment strength and perpendicular to grain stresses. Fastener embedment behaviour varies between panel types and orientation requiring special attention on the part of the designer. Platform construction detailing (Figure 16) tends to reduce issues embedment and perpendicular to grain stress issues since floor loads are transferred into vertical elements through bearing, however transferring of vertical loads from the element above the panel to that immediately below it introduce a new set of problems. In balloon construction, these issues are reversed (Figure 16).

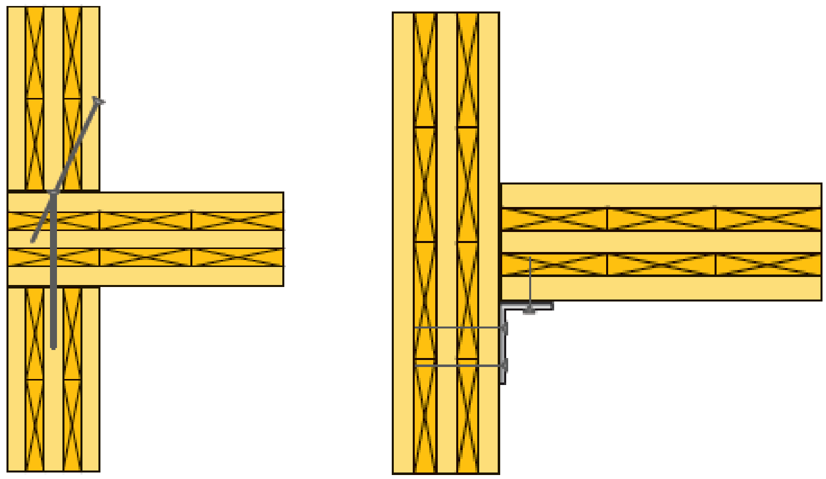

Figure 16: Timber panel connections in platform (left) and balloon (right) construction (FPInnovations)

The simplest method of timber panel – steel beam connection is achieved by bearing panel ends on steel beam flanges with fasteners screwed through drilled flange holes. To this end, I-beams and channels are ideal candidates for perimeter beams and girders as they provide a natural landing place for floor panels. This system is beneficial from an erection standpoint since prefabricated panels can be flown in and quickly slotted into place with no temporary supports or fastenings required. Panels can be rested on either top or bottom flanges where I-beam girders are used. Placing panels on bottom flanges serves to limit overall floor depth while panels rested on top flanges allow for continuous floor spans. Top flange placement has the added benefit of potentially increasing the stiffness properties of the steel beam through composite behaviour, an item discussed further in Section 0. There are several means of fastening floor panels to steel sections. One method for securing panels to beams is through screws inserted through the steel flange perpendicular to grain into the wood section element. These shear connectors are individually installed through pre-drilled holes in the flange after the panels have been placed. Examples of panels placed and fastened to flanges is shown in Figure 17. Alternatively, metal brackets as shown in Figure 18 can be used to fasten panels to beams and wall elements.

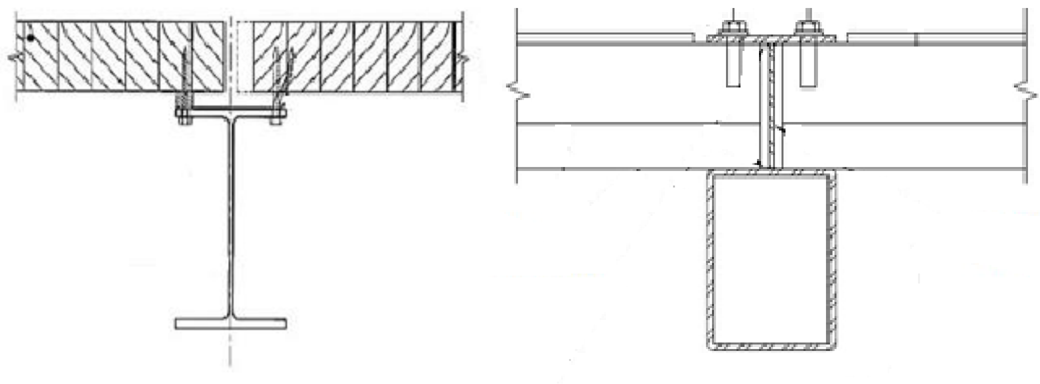

Figure 17: Nail-laminated panels fastened through bottom flange (Scotia Place) and through top flange (Fast + Epp Structural Engineers)

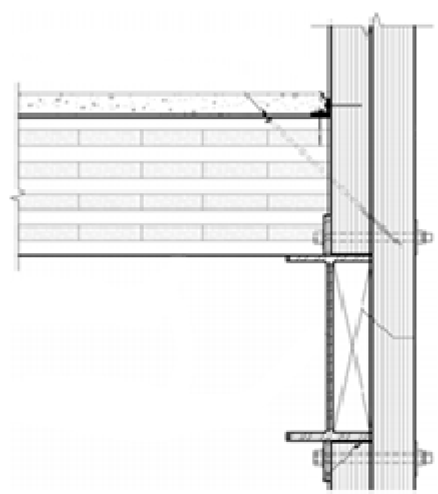

Figure 18: Top-mounted CLT floor panel fastened to wall via angle brackets (Equilibrium Consulting Inc.)

Figure 19: Examples of mass-timber panels mounted on bottom flanges of steel framing (Fast + Epp Structural Engineers)

Design of panel-beam end connections for vertical loading is relatively straightforward. Bearing capacity requirements are not difficult to attain given panels are continuously providing ample bearing area. Panel depth will often be governed by serviceability criteria which may place emphasis on achieving some measure of connection fixity to reduce floor vibrations. Flange-panel fastener spacing is dictated by lateral load demands and the orientation of load relative to wood grain. In this case nail-lam and glulam panel floors are loaded perpendicular to grain while CLT layers are both loaded perpendicular and parallel to grain. CSA 086 provides guidance for connection of nail and glue-laminated panels for all loading and orientations. A more comprehensive reference for connections using CLT elements is the CLT Handbook produced by FPInnovations.

In addition to fastener and panel design, steel beams supporting panel ends must also be checked for global bending and shear capacity as well as transverse flange bending. Since shear forces are transferred into the steel beam through bearing on top or bottom flanges, bending about the longitudinal axis of the web resulting from the eccentricity between the panel end and the steel web must be considered. Steel beams may require detailing preventing rotation due to asymmetrically loaded flanges, in particular at perimeter girders. Excessive rotations can lead to loss of bearing area and additional stresses on shear connectors. Alternatively, the right image of Figure 17 demonstrates a detail which eliminates flange bending and rotation about the longitudinal axis by providing a built-up I-section where the panel rests on the top wall of an HSS section.

3.2 Design Considerations

This section discusses several aspects of design unique to timber floor – steel frame hybrid structures. The topics covered here do not encompass every issue involved in timber-steel hybrid structures but rather cover a few pertinent aspects of relevance to designers.

3.2.1 Composite Behaviour

Where timber panels are used as continuous spans over intermediate steel floor beams they are fastened by means explained in the previous section, theoretically producing composite beam behaviour. Composite behaviour of joisted floors in steel frames is not considered to be significant and is hence disregarded here. Composite behaviour is commonly used in steel-frame concrete-deck applications to increase strength and stiffness. Clause 17 of S16-01 describes the available increase in moment resistance and stiffness for steel-concrete composites as a function of the shear connection between the materials. Composite behaviour is also used in timber construction where 50-100 mm of concrete topping is used to reduce deflection, vibration, and sound transmission.

However the use of timber flooring as a means of increasing the bending capacity of steel sections is not as common. First, for nail and glue-laminated panels, the orientation is such that their longitudinal axis is perpendicular to the longitudinal axis of the supporting steel beam. If these elements are to be considered for composite action, assuming full shear connectivity between steel and wood, compressive stresses will be applied perpendicular to the grain where the capacity of a No.1/No.2 grade D.Fir-Larch board is 7.0 MPa (CSA 086). The elastic modulus in the radial direction of sawn lumber is estimated to be 6.8% that of the elastic modulus in the longitudinal axis (11000 MPa by CSA 086), amounting to a stiffness less than 1% that of structural mild steel (Green, Winandy, & Kretschmann, 1999).

In light of the discrepancy in elastic moduli, research related to wood-steel composite behaviour is limited. Composite behaviour would only be reasonable where large timber sections are augmented by thin steel sections. Where an entire steel I-beam cross-section is used, the strength and stiffness tends to dwarf the contributions of the wood section. In real building applications where timber panels run continuous over steel beams designers consider the available stiffness of the steel section alone for simplicity.

3.2.1.1 CLT-Steel Composite Behaviour

Whereas the orientation of nail and glue-laminated panels does not create efficient composite behaviour due to the low elastic modulus perpendicular to the grain, CLT panels always have at minimum one layer of wood orientated parallel to the steel beam where the stronger elastic modulus parallel to the grain can be taken advantage of. The investigation of the potential increases in beam-panel stiffness is then merited.

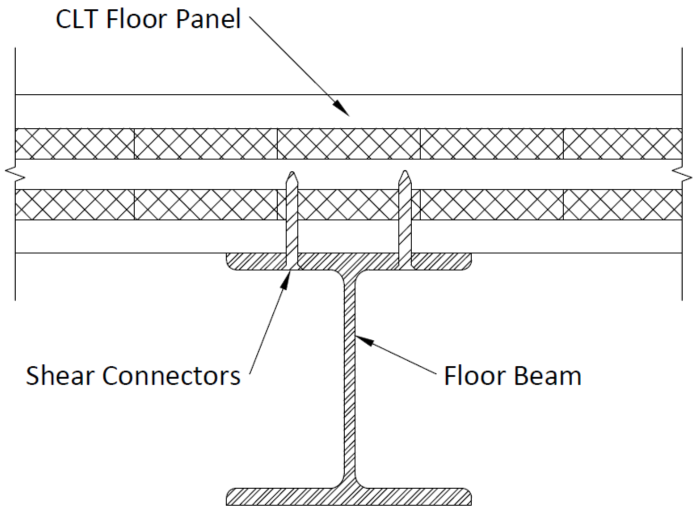

Figure 20: Steel-CLT composite beam

The main issues associated with composite behaviour of steel-CLT beams include shear connectivity, effective CLT width, and calculation of CLT stiffness. To achieve efficient composite behaviour, fasteners connecting both materials must be able to provide adequate strength and stiffness. Connector type, diameter, embedment length, spacing, initial slip, and embedment angle will heavily influence the behaviour of the composite section. As mentioned, experimental data regarding these parameters is lacking. Effective CLT width will also influence the composite behaviour available. For comparison, the handbook of steel construction recommends effective width of steel-concrete composite floors be taken as either one quarter the length of beam span or the average spacing of parallel steel beams. The effective width is a function of the ability of the section (concrete or wood) to transfer longitudinal shear stress as far outwards (horizontally) as possible. In CLT this is achieved mechanically. Laminations parallel to the steel beam, those providing stiffness, though they may not be edge glued and transfer shear thusly, are connected by perpendicular laminations above and below. The effectiveness of these laminations in transferring longitudinal shear will greatly influence the effective width and composite behaviour of steel-CLT section.

The final issue, calculating CLT stiffness, has no universally accepted method. The CLT Handbook presents several different possible approaches for designers to employ. The difficulty in determining the bending properties of CLT lie in the fact that not all layers are oriented in the same direction and the stiffness of the laminations is orthotropic, resulting in discontinuous stress distribution over the panel cross section. The composite theory approach is one method used for determining the effective strength and stiffness of cross-laminated elements. (Blass & Fellmoser, 2004) The method proposed by Blass and Fellmoser does not take shear deformation into account, making it practical in floors with large span-to-depth ratios. The theory uses "composition factors" (k-factors) to relate the strength or stiffness of orthogonal layers for determining the stress distribution along the cross section. Using a ratio of elastic moduli parallel to the grain versus perpendicular to the grain as $E_0/E_{90} = 30$, the composition factors in Table 5 are calculated to evaluate effective strength and stiffness values for the CLT element under various loading types.

Table 5: Composite method composition factors for CLT bending capacity (Blass & Fellmoser, 2004)

	k_i
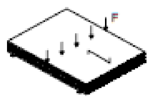	$k_1 = 1-\left(1-\frac{E_{90}}{E_0}\right)\cdot\frac{a_{m-2}^3 - a_{m-4}^3 + \ldots \pm a_1^3}{a_m^3}$
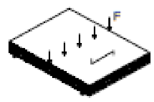	$k_2 = \frac{E_{90}}{E_0}+\left(1-\frac{E_{90}}{E_0}\right)\cdot\frac{a_{m-2}^3 - a_{m-4}^3 + \ldots \pm a_1^3}{a_m^3}$
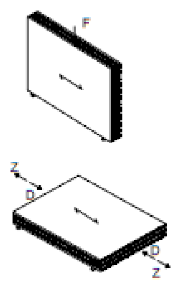	$k_3 = 1-\left(1-\frac{E_{90}}{E_0}\right)\cdot\frac{a_{m-2} - a_{m-4} + \ldots \pm a_1}{a_m}$
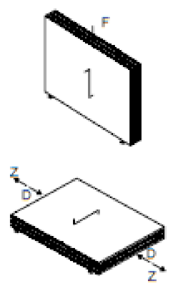	$k_4 = \frac{E_{90}}{E_0}+\left(1-\frac{E_{90}}{E_0}\right)\cdot\frac{a_{m-2} - a_{m-4} + \ldots \pm a_1}{a_m}$

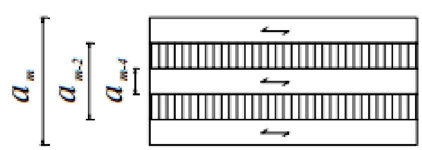

Table 6: Effective strength and stiffness values using composite factors (Blass & Fellmoser, 2004)

Loading	To the grain of outer skins	Effective strength value	Effective stiffness value
Perpendicular to the plane loading			
Bending	Parallel	$f_{m,0,ef} = f_{m,0} \cdot k_1$	$E_{m,0,ef} = E_0 \cdot k_1$
	Perpendicular	$f_{m,90,ef} = f_{m,0} \cdot k_2 \cdot a_m / a_{m-2}$	$E_{m,90,ef} = E_0 \cdot k_2$
In-plane loading			
Bending	Parallel	$f_{m,0,ef} = f_{m,0} \cdot k_3$	$E_{m,0,ef} = E_0 \cdot k_3$
	Perpendicular	$f_{m,90,ef} = f_{m,0} \cdot k_4$	$E_{m,90,ef} = E_0 \cdot k_4$
Tension	Parallel	$f_{t,0,ef} = f_{t,0} \cdot k_3$	$E_{t,0,ef} = E_0 \cdot k_3$
	Perpendicular	$f_{t,90,ef} = f_{t,0} \cdot k_4$	$E_{t,90,ef} = E_0 \cdot k_4$
Compression	Parallel	$f_{c,0,ef} = f_{c,0} \cdot k_3$	$E_{c,0,ef} = E_0 \cdot k_3$
	Perpendicular	$f_{c,90,ef} = f_{c,0} \cdot k_4$	$E_{c,90,ef} = E_0 \cdot k_4$

Since little research has been done to quantify connector stiffness and effect on composite behaviour of timber-steel composite beams the two extreme cases, no composite behaviour and full composite behaviour, are considered here to assess the available range of stiffness. The calculation of bending stiffness must then be calculated two separate ways. For fully composite behaviour it is assumed that the entire CLT section is in flexural compression and hence composite factor k_4 is used to calculate effective strength and stiffness. When considering no composite behaviour the factor k_2 is used.

Table 7 shows the increase in bending stiffness that can be achieved when full composite behaviour is achieved in CLT-steel composite beams. Calculations are performed using a W250x101 CISC section and considering an effective CLT width of 500mm. Elastic modulus values for the CLT sections are calculated according to the previously mentioned composite factors and equations in Table 6.

Table 7: Effects of CLT-steel composite behaviour

CLT	CLT E_{90} (MPa)	No Composite $\Sigma(EI_{CLT} + EI_{steel})/EI_{steel}$	Full Composite $EI_{composite}/EI_{steel}$	Percent Increase (%)
3-ply	3366	1.00	1.32	32
5-ply	4060	1.01	1.44	43
7-ply	4368	1.05	1.85	76
9-ply	4542	1.11	2.41	117

Table 7 shows that a conservative assumption of no composite behaviour being present in CLT-steel beams yields at best an 11% increase, using 9-ply panels, in stiffness beyond what is provided by the steel alone. Results for 3, 5 and 7-ply panels are below 5% increase, demonstrating the disparity between elastic modulus of the two materials. The other extreme case, full composite behaviour, yields increases between 32-141% beyond what is offered by the steel alone, and 32-117% beyond what is offered by the sum of steel and CLT stiffness. Considering the most optimistic result for developing composite behaviour between timber and steel will be less than 100% connectivity, the results from Table 7 show that significant composite benefit is only achieved where larger panel sizes are used. The results from Table 7 are for one steel section and an assumed effective width. Where smaller steel sections are used and more effective width is shown to be available, the values for increase in stiffness due to the CLT can go beyond what is shown in the table.

Research is required to assess the connector parameters, establish the composite behaviour and failure mode (connector yielding or local wood bearing failure), and composite behaviour of butt-jointed panels at steel beam locations.

3.2.2 Lateral Bracing

Where wood-based flooring is used within steel floor framing, it may be desirable to the employ the flooring as lateral bracing of steel sections as well. In the case of joisted floors, web-mounted ledgers complete with joist hangers as shown in Figure 9 can provide restraint to both top and bottom flanges, eliminating the need for steel bridging entirely. Where top mounted joist hangers are used (Figure 11), lateral support is not provided for the bottom flange. Timber panel floors, unlike face-mounted joisted floors, are only capable of providing lateral support to either the top of bottom flange. Whereas lateral support from joists is provided through bearing contact surface at the joist end, panel floors must rely on shear connectors to transfer load from beam to panel. Clause 9.2.7 of S16-01 states that if a slab or decking is used to brace the compressed flange of steel beams the slab/deck must be able to resist 5% of the maximum force in the flange or chord. This extra force should be added in the gravity analysis of wooden floors within steel beams.

3.2.3 Structural Weight

One of the primary benefits to incorporating wood-based floors in steel construction is for floor weight reductions leading to smaller member sizes and foundations resulting in potential cost savings. To assess the veracity of this claim a summary of floor weights for a range of wood-based flooring options is calculated using CSA 086 member design for single, double and triple span floors. Live load and partition load are calculated based on NBCC loading for residential structures. The assumed material/member densities are found in Table 8.

Table 8: Summary of wood element densities

Material/Member	Density (kg/m³)
Sawn Lumber[1]	420
Engineered Joists[2]	3.4-6.0[2]
Nail-laminated Panel[1]	420
Glulam Panel[3]	440
CLT[3]	500
Plywood[4]	500
Concrete	2450

[1]CSA 086
[2]Weyerhaueser, (kg/m)
[3]StructurLam
[4]CANPLY

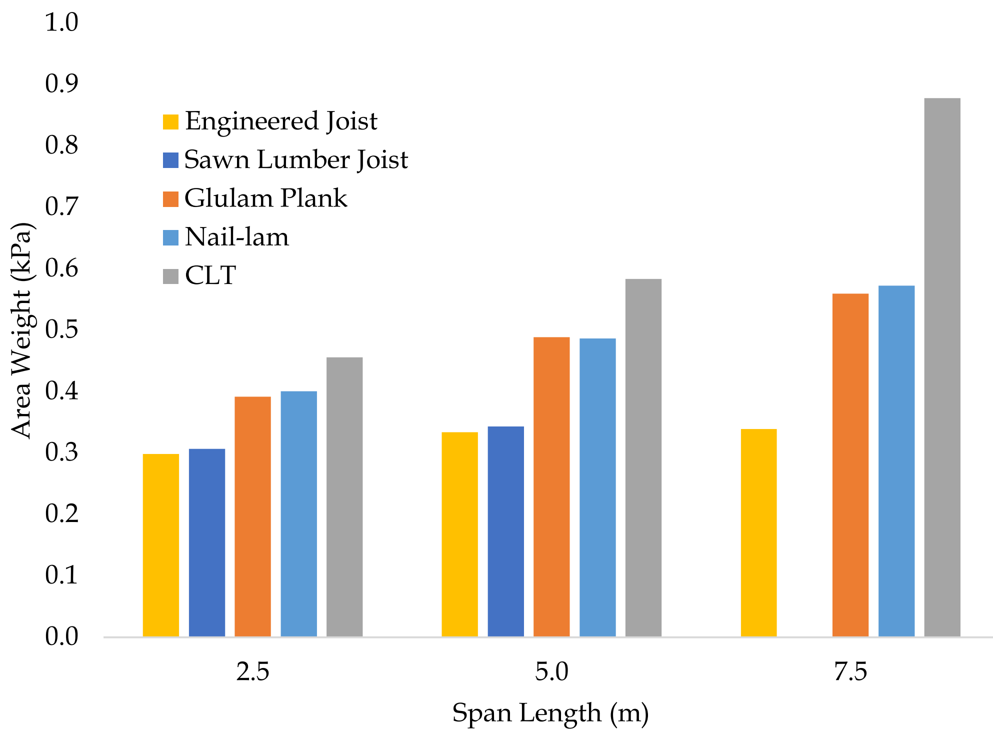

Figure 21: Area weight for single span floors relative to equivalent concrete floor

Figure 21 shows the area weights for three different span lengths divided by the equivalent concrete weight required to achieve the span. Span lengths as multiples of 2.5 m are chosen to accommodate the building dimensions. Figure 21 shows all flooring options are below 1.0, meaning each option is lighter than the equivalent concrete option. It is apparent from the figure that engineered joists provide the lightest spanning solution for single-bay simply supported floors. CLT is the heaviest option at each span length, in particular at 7.5 m span lengths since 9-ply (309 mm deep) panels are required. Sawn lumber joists are not available in 7.5 m lengths (Table 9), hence their exclusion from 7.5 span length section in Figure 21, though at 2.5 m and 5.0 m span lengths they compare favourably against the other floor options. Figure 21 also shows that joisted floors are superior to panel floors when it comes to self-weight. In terms of optimal span lengths, it appears that the shorter the span the greater the weight savings, though shorter simple spans result in more intermediate beams, their weight and added cost is not accounted for in the figure.

Flooring systems are constricted by the maximum commercially available element lengths. Table 9 lists the maximum lengths available in British Columbia. Lengths for EJ, CLT and glulam are based on individual suppliers. From the table we see that in addition to providing the lightest option, EJ can accommodate the largest spans in comparison to the other four options.

Table 9: Summary of available element lengths

Element	Available Length (m)
Sawn Lumber	7.25
Engineered Joists	18.30
Nail-laminated Panel	custom
Glulam Panel	custom
CLT	12.20

[1] Panels made of sawn lumber - no length limit

It can be beneficial to span elements across multiple supports to reduce the deflection demands (2 and 3 spans are better than 1), or reduce the moment demand (3-span is better than 1-span). Reducing the amount of spans also reduces the amount of required connections and can speed up erection time.

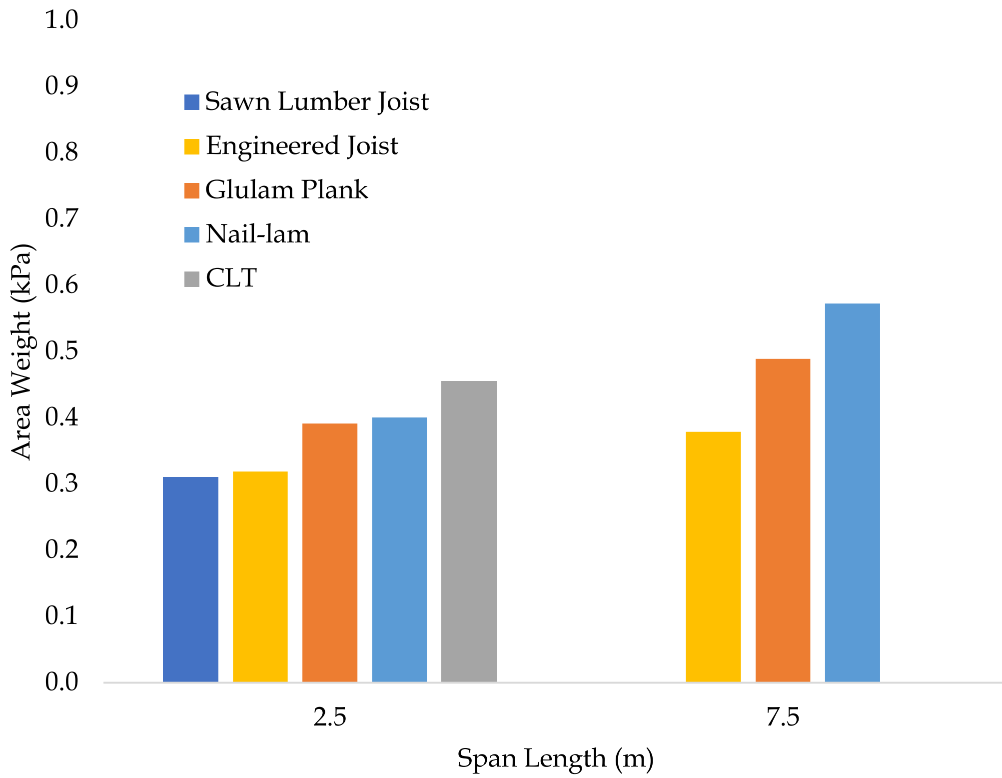

Figure 22: Area weight for double span floors relative to equivalent concrete floor

From Figure 22 shows that for double span floors engineered and sawn lumber joists provide the lightest solution, though all five flooring remain significantly below the equivalent concrete floor. At 7.5 m span lengths sawn lumber joists and CLT floors are no longer an option due to available lengths (Table 9). Once again, as was seen in single span weights, the shorter span lengths produce lighter floor weights.

Figure 23: Area weight for triple span floors relative to equivalent concrete floor

Figure 23 shows floor weights for triple span floors. 7.5 m floors are not considered since this would require joist/panel lengths of 22.5 m, which are not commonly seen and hence excluded. The results indicate that sawn lumber and engineered joists once again provide the lightest flooring option, with glulam and nail-lam planks roughly 26% heavier, and CLT 48% heavier. Also, as was seen in single and double spans, the shorter span produces lighter floor weights.

Comparison of the three figures shows that single, double or triple (continuous) spans of 2.5 m span lengths produce the lowest area weight for each floor spanning element. While it is advantageous to minimize span lengths regardless of the material type, this increases the amount of beams (and possibly columns) and connections required. When compared with an equivalent concrete floor, all wood-based flooring options indicate significant reductions in overall floor weight, validating the motivation for including wood-based floors in steel frame structures.

3.2.4 Floor Vibration

3.2.4.1 Performance of Typical Floor Systems

One of the main concerns for tenants in multi-unit residential structures is floor vibration. Units in concrete buildings are often valued higher than their wooden counterparts under the assumption that the former provides superior vibration damping and noise suppression. Wood-based floors have less self-weight than most flooring types, concrete slabs for instance, and higher fundamental frequencies. Though the issue of vibrations in all floor types has been investigated extensively, codebooks often present methods for analysis and design as recommendations rather than definitive solutions due to the highly subjective nature of the issue.

Wooden joisted floors are lightweight and usually have frequencies greater than 15 Hz. A traditional method, and one still used today, for determining vibration controlled span lengths is based off the ability of the floor to keep deflections below 2 mm when loaded with a 1 kN point load at mid-span. This method is included in the 2005 NBCC. This method is not comprehensive in that it neglects damping and the influence of extra area masses such as concrete topping or other non-structural components. (FPInnovations, 2011)

Alternatively, approaches based on frequencies of floor vibration have been suggested for use in lightweight joisted floors. Researchers at Virginia Tech University proposed an equation to calculate the fundamental frequency of a floor system based on the natural frequencies of individual elements making up the system. The equation neglects material damping, additional floor weights (carpets, cabinets etc.) and composite benefit provided by plywood sheathing and gypsum ceiling panels, using only structural dead load (topping not included). The equation for natural joist/girder frequency is also based on static deflection of the element and is shown in [1] and [2]:

$$f = \frac{\pi}{2}\sqrt{\frac{EIg}{WL^3}} \quad [1]$$

$$f = \sqrt{\frac{f_{joist} * f_{girder}^2}{f_{joist} + f_{girder}^2}} \quad [2]$$

(Nolan, Murray, Johnson, Runte, & Shue, 1999)

While the equations can provide a suitable estimate for natural frequency the influence of the previously mentioned factors must be accounted for to produce a more robust method of calculation.

A method developed by scientists at FPInnovations was originally intended for joisted floors but was later verified as eligible for use in mass timber panels as well. Timber panels have greater area mass (30-150 kg/m²) and a lower natural frequency (9 Hz) than joisted floors. The method proposed also employs both static and dynamic components mentioned previously to produce a design equation based on the material properties to calculate a maximum vibration controlled span length. The equation adopted for cross-laminated panels is seen in [3].

$$l \leq \frac{1}{9.15}\frac{(EI_{eff}^{1m})^{0.293}}{(\rho A)^{0.123}} \quad [3]$$

(Hu & Gagnon, 2012)

One difficulty in this approach is the calculation of effective stiffness for a 1 m CLT panel in the strong orientation. Different methods exist for this calculation resulting in different conclusions. While it is not yet a comprehensive equation for all floor types, joisted or panel, and all practical area masses, it is perhaps the most promising method available to designers currently. (Hu & Gagnon, 2012)

Most floors in steel construction consist of floor beams or joists carrying a concrete deck between parallel steel girders. These floors have high area masses (>200 kg/m²) and low natural frequencies (<9 Hz) when compared with joisted and panel wood floors. The approach to floor vibration in steel construction is similar to the proposed method for CLT panels whereby static deflection is used to determine the natural frequency of joist and girder elements which are then combined to determine the total floor frequency. Unlike the previous method which incorporates panel deflection due to a single point load, this approach uses the deflection of the entire applied load as a uniformly distributed load when calculating the natural frequency of the floor:

$$f_n = \frac{\pi}{2}\sqrt{\frac{gE_sI_t}{wL^4}} \qquad [4]$$

$$f_n = 0.18\sqrt{\frac{g}{(\Delta_j + \Delta_g)}} \qquad [5]$$

(Murray, Allen, & Ungar, 2003)

To account for composite behaviour between the two materials creating a stiffer section than the steel element alone, a transformed moment of inertia is used in the element frequency calculation as well as in the deflection calculation. To account for different stiffnesses of joists and girders, individual deflections are combined as shown in [4] and [5] to represent the overall floor performance. Continuous spans are also often used in steel construction to reduce deflections, a configuration which may affect the vibration performance of a floor. Adjacent spans deflect in opposite vertical directions due to the influence of intermediate support and thus for spans of equal length the calculated displacement will be equal that for a static simply supported beam. Modifications to the deflection calculation must be made where adjacent span lengths are unequal. (Murray, Allen, & Ungar, 2003)

A study conducted on hybrid steel truss-LVL panel floors by FPInnovations investigated appropriate methods for floor vibration design using both the steel-concrete approach by Murray, Allen & Ungar as well as the lightweight joisted floor approach by FPInnovations. The floors in question had area masses between 30-40 kg/m^2, much closer to the 20 kg/m^2 used in the wood method rather than the 200 kg/m^2 used in the steel method. The researchers found the steel approach not suitable for predicting floor vibrations due to the large discrepancies in recommended weight and sensitivity to damping ratios, a difficult parameter to estimate for new flooring systems. It was determined by the researchers that the wood design method which used static deflection values to calculate natural frequencies as a suitable method of estimating floor vibration.

As has been shown in the reviewed literature, floor vibration is largely dependent on floor mass. To this end, it would appear that wood panel design method [3] is most suitable for timber-steel hybrid floors. Results from Section 3.2.3 demonstrate that hybrid timber-steel floors weigh far less than their concrete and steel-concrete composite counterparts. However in instances where floor weight in timber-steel hybrid floors approaches concrete floor values (deep, long CLT floors with topping as seen in Figure 21), the steel-concrete composite method in [4] & [5] may be preferable. Joisted floors framing into web-connected rimboards as seen in Figure 9 can be analysed similar to [4] & [5] where different joist and girder stiffnesses are calculated though the timber deflections will significantly outweigh steel deflections for the given spans. End conditions for joisted construction can generally be regarded as pinned since joist hangers are flexible and nail yielding and wood crushing will rarely result in a fixed beam condition. Span continuity and composite behaviour can also be considered as previously mentioned.

Though exact values for vibration of wood-based floors vary, the effect of steel framing on the vibration of timber floors is not overly influential and in most cases design methods used to control vibration in entirely wood-based structures can be used for hybrid timber-steel structures.

CHAPTER 4: **SEISMIC LOADING**

4.1 Background

Ground motions from seismic events cause lateral accelerations of building mass creating inertial forces which must be resisted by a structures SFRS. Shear walls, moment frames and braced frames are three common methods of providing lateral strength to structures vulnerable to seismic activity. A large portion of structural mass is distributed over the floor area and when accelerated the resulting inertial forces must be transferred to the SFRS. The action of a floor transferring inertial forces to the SFRS is known as diaphragm action. Seismic loading on diaphragms is treated as a horizontal uniformly distributed load resulting in bending and shearing forces developing along the length of the floor.

In-plane stiffness is the most important property of a diaphragm affecting both the lateral distribution of forces to designated lateral force elements, as well as the torsional demand on a structure. For the purpose of simplifying analysis diaphragm stiffnesses are conventionally separated into two categories: rigid or flexible. Where the rigid diaphragm assumption is made, forces are distributed to vertical supports (walls or frames) according their respective stiffnesses. Where a flexible diaphragm assumption is made, forces are distributed according to their respective tributary floor area, similar to the pin-supported bending beam problem. The corollary to distribution of lateral forces is torsional demand. In the event of an eccentricity between the centres of rigidity and mass, a rigid diaphragm will rotate about the centre of rigidity creating additional lateral demand on the SFRS whereas a flexible diaphragm has no tendency to rotate. The additional demand placed on the SFRS is reflected in the 2010 NBCC list of irregularities under torsional sensitivity when a diaphragm is considered not flexible.

The International Building Code (IBC) (ASCE 7-05 12.3.1 as well) allows designers to determine the rigidity of a diaphragm based on the ratio of in-plane deflection to the drift of the associated storey. Where the in-plane diaphragm deflections are less than twice the storey drift a diaphragm can be considered rigid. Though restrictions and amendments based on building type and size have been added to this clause in the IBC, this remains a viable method of determining diaphragm flexibility. As will be further discussed, the relative stiffness of diaphragm to storey is a common method for determining diaphragm classification for several different construction methods. Though advanced modeling with specific stiffness can accurately determine the real distribution of forces in a structure with asymmetric SFRS and semi-rigid diaphragms, this requires detailed elastic and inelastic mechanical properties and non-linear analysis, this task is difficult and time consuming and may be impractical in design of mid-rise residential structures. As a result the method of relative stiffness and the IBC requirement will be used here to determine the flexibility of hybrid diaphragms.

Once the in-plane stiffness of a diaphragm has been assigned two common methods of determining distribution of lateral forces are used, the tributary area method for flexible diaphragms and the stiffness method for rigid diaphragms. The tributary area method equation, derived from statics, is as follows:

$$F_i = \left(\frac{A_i}{A}\right) F \qquad [6]$$

Where F_i is the lateral force demand on support i, F is the total lateral diaphragm force assuming uniform distribution, A_i is tributary area of support i, and A is the total diaphragm area.

The stiffness method uses structural matrix analysis to determine lateral force distribution. A local stiffness matrix typically with two translational degrees of freedom and one rotational, is defined for each support as well as transformation matrices to convert from local to global coordinates. The global stiffness matrix is achieved by the summation of all transformed support matrices. Once the global force vector has been established the force-deformation relationship, $\hat{F} = \boldsymbol{k}\hat{u}$, can be rearranged to solve for the global deformation vector,

$\hat{u}$. Finally, the force on each support can be obtained by multiplying the global stiffness matrices of each support by the global deformation matrix. A more comprehensive description can be found in structural analysis texts.

The following sections discuss approaches to the issue of determining diaphragm stiffness in wood, steel and hybrid construction and investigating the influence of each of the lateral force distribution and torsional demand on mid-rise residential structures.

4.1.1 Wood Construction

4.1.1.1 Joisted Floors

In-plane stiffness of wooden joisted floors is achieved through plywood sheathing fastened on top of joists using nails, screws, glue or a combination thereof. This system, with intermediate blocking at free panel edges, provides stiffness and strength regardless of the orientation of the joists relative to the applied load. The performance of lightweight joisted floors is a function of plywood panel arrangement, plywood species and thickness, nail size and spacing, extent of blocking, aspect ratio and perimeter framing.

For analysis purposes joisted floors are often considered to behave similar to an I-beam where perimeter framing elements, chords, perpendicular to the applied load act as flanges to resist bending and the plywood sheathing acts as the web in resisting shear forces. In keeping with this analysis, the CSA 086 design code uses four terms to calculate deflection of wood diaphragms.

$$\Delta_d = \frac{5vL^3}{96EAL_D} + \frac{vL}{4B_v} + 0.000614Le_n + \frac{\sum(\Delta_c x)}{2L_D} \qquad [7]$$

The equation represents four separate actions contributing to deflection of diaphragms treated as uniformly loaded simply supported beams. The four terms, in order, relate to flexural deflection of the chords, shear deflection of the panels, panel edge movement and chord-splice slip. The flexural term is an algebraic manipulation of the classical Euler-Bernoulli beam bending equation that only gives credit for the moment of inertia of the two chords and conservatively neglects both the individual chord moments of inertia as well as the contribution from the plywood. Chord area, A , can be taken as the area of perimeter rim joists or the area of the double top plate of the wall below, whichever is provided and meaningfully connected to the diaphragm. The shear deflection term is a similar manipulation rearranged to express the deflection as a function of maximum shear force on the diaphragm averaged over the area parallel to the direction of load. Shear stiffness term, B_v, provided in the standard is a function of sheathing species and thickness. The panel edge movement term is a function of the nail load-slip behaviour at panel edges, summarized in the empirically formulated third term. Some standards consider panel edge movement and shear deflection as one action and the two terms are consolidated; 086 chooses not to. The final term, chord-splice slip, is included in anticipation of axial displacement at butt-ended joints. Typical chords are made up of two 2x8″, 2x10″, or 2x12″ pieces of 8′-20′ lengths with alternating splices. Chords loaded in tension will undergo slip from nail deformation while it is assumed that chords in compression can also slip an amount equal to the gap between consecutive lumber pieces. Deflection of chorded diaphragms, unblocked or blocked, are similar to deep beams where shear deflection governs overall deflection. This observation is reflected in Figure 24, comparing the various contributions to diaphragm deflection where panel edge movement is included in the shear deflection term. Deflections are calculated based on CSA 086 design provisions. As is evidenced in the figure, flexural deflections only become significant at aspect ratios of two, increasing by the cube of span length and behaving less like a deep shear beam. The figure also demonstrates the negligible impact of chord-splice slip deflection. (Bott, 2005)

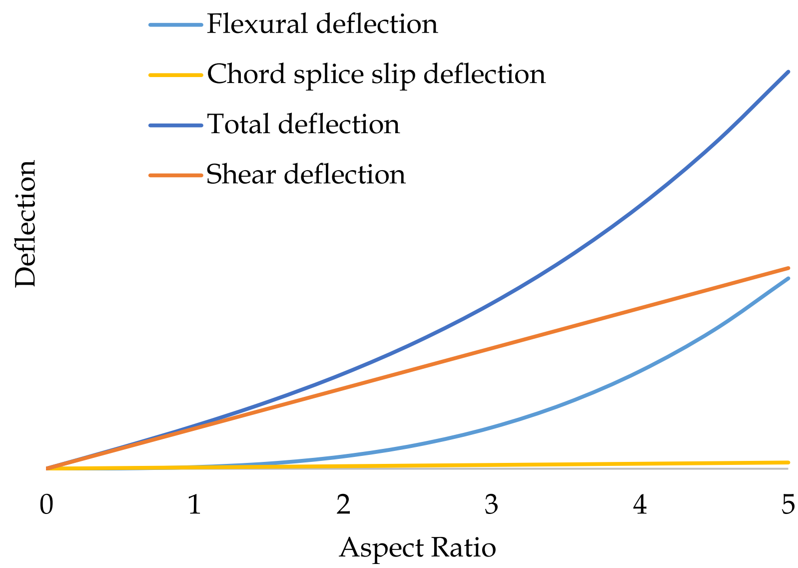

Figure 24: Contributions to diaphragm deflection using design provisions

As mentioned, wood diaphragms have been traditionally treated as flexible, and the distribution of lateral forces into walls was considered to be based on tributary area. Before the use of plywood became overwhelmingly popular in North American residential structures, diagonal planks, or diagonal lumber sheathing, were nailed over wooden joists to provide a flooring surface. This flooring type predated the earthquake demands seen in current codes at a time when lateral performance of structures was mostly considered for wind loading only. Diaphragms were conservatively estimated to be flexible since strict nail spacings were not prescribed and minimal research on in-plane stiffness of joisted floors had been done.

Research in recent decades has begun to challenge the assertion that joisted diaphragms should be considered flexible. Testing done by Filiatrault, Fischer, Folz and Huang in 2002 showed that many joisted floors with typical blocking and nail spacings would be considered rigid under Uniform Building Code provisions which state that diaphragms are to be considered rigid where in-plane deflections are less than twice the storey drift of the appropriate storey. (Filiatrault, Fischer, Folz, & Uang, 2002) Testing on multiple diaphragm configurations varying parameters such as aspect ratio, chords, blocking, and adhesives demonstrated that wooden diaphragms could exhibit excellent in-plane stiffness. (Bott, 2005) Further analysis by (Huang, 2013) using the results from Bott's testing showed that in lieu of forcing a rigid or flexible designation, wood diaphragms are mostly semi-rigid. Huang argues that more important to lateral force distribution is the relative stiffness of diaphragms to walls. While a diaphragm may have a certain stiffness from which it could be designated as rigid or flexible, the distribution of lateral forces is more significantly impacted by the difference in stiffness of the wall and diaphragm.

4.1.1.2 Panel Floors

Individual timber panels can provide excellent in-plane stiffness. The cross-laminations in CLT panels allow for excellent in-plane stiffness in all directions while nail-laminated panels require supplementary sheathing to ensure stiffness can be achieved in the direction parallel to the laminations. As individual elements, CLT panels can be considered rigid, however the stiffness properties change when connecting multiple panels to make up a complete diaphragm. There are many methods for panel connection though in most practical scenarios it can be assumed that the connection stiffness is less than the panel in-plane stiffness. As a result the majority of in-plane diaphragm deformation is a result of slip between adjacent panels. Research has shown that though the in-plane performance of individual CLT panels is quite rigid, multiple connected panels tend to behave in a flexible manner. The behaviour of connected CLT panels loaded perpendicular to the connected edge are likely to behave similar to a single panel since splice connections can provide shear transfer allowing for full composite behaviour of all panels. Once again, though the individual stiffness of CLT diaphragms is important, the governing factor in the distribution of lateral loads is relative stiffness between diaphragm and supporting elements. (Ashtari, 2009)

The IBC method of determining floor flexibility based on the comparison of diaphragm and storey drifts as is done for lightweight floors has not been verified for CLT diaphragms. In lieu of further research on this topic it is recommended that designers perform computational modeling to assess the distribution of lateral forces to diaphragm supports.

As mentioned, nail-laminated panels achieve stiffness in both directions through overlain sheathing, supplemented by shear stiffness of sawn lumber boards in the perpendicular to spanning direction, and by nails driven through adjacent boards in the parallel to spanning direction. While CLT diaphragms rely on panel-edge connections to achieve overall diaphragm behaviour, which has been shown to be flexible, adjacent nail-laminated panels are connecting by overlapping sheathing creating a floor type similar to lightweight floors. In light of joisted sheathed floors being considered semi-rigid, nail-laminated floors can be reasonably assumed to behave semi-rigid, if not entirely rigid based on the additional shear stiffness provided by the edge-laminated sawn lumber boards. Further research on this matter is required.

4.1.2 Steel Construction

Floors in steel construction consist of light-gauge steel decking topped with several inches of reinforced concrete and typically span between beams spaced 2-4 metres apart. Behaviour of these composite floors under lateral loading is analysed as an I-beam where the steel perimeter chords are stressed in bending and the deck in shear, just as is done in wood joisted floors. The continuity of the reinforced concrete deck provides excellent shear stiffness and hence unlike wood joisted floors, composite diaphragms are often considered to be rigid, though ultimately the aspect ratio governs this assertion. (Metten, 2011) The mid-span deflection of composite diaphragms can be calculated by the following equation:

$$\Delta = \frac{5WL^4}{384EI} + \frac{q_{avg}(\frac{L}{2})}{G'x10^6} \qquad [8]$$

(CISC, 2006)

Where the first term considers the flexural deflection considering the bending stiffness of the chords alone, while the second term considers the shear deflection of the deck where G' is the shear flexibility of the deck as a function of connectors, thickness, profile and resistance to warping.

In steel construction, as with all other methods previously discussed, the distribution of lateral forces a function of the relative stiffness of the diaphragm and SFRS. The limiting 2:1 ratio of mid-span diaphragm deflection to storey drift for assessing diaphragm flexibility is applicable in composite decks as well. Though for simplification purposes composite decks are often treated as rigid, a semi-rigid case may exist in which case computer modelling would be recommended for designers calculating the distribution of lateral forces. Conservatively, an envelope of maxima from both the rigid and flexible assumption could be used.

4.1.3 Hybrid Construction

While the performance of hybrid timber-steel floors has not been extensively researched, the precedent set by several relevant works provides guidance. In the case of steel perimeter framing with infill joisted floors the in-plane behaviour is best determined in a similar fashion to all-wood joisted floors. Where framing detailing is similar to that shown in Figure 9, where web-fastened ledgers are capable of transferring shear forces into the steel perimeter beam, the I-beam analogy used for joisted wood floors is relevant, though global diaphragm stiffness is unlikely to be significantly impacted. The contributions to diaphragm deflection shown in Figure 24 demonstrates that these flooring systems are dominated by shear deformation for floor aspect ratios below 3:1 and hence the substitution for a substantially stiffer section (steel I-beam vs. sawn lumber board) will not greatly affect the behaviour. Experimental work on joisted diaphragms by Bott demonstrated that the presence of wooden chords can increase flexural stiffness by 154% while only providing 40% increase in cyclic stiffness, suggesting that diaphragms are stiff in flexure compared to shear even without perimeter chords. (Bott, 2005) In addition to this, research by Li et al. showed the in-plane stiffness of bare steel frames is essentially flexible and infilling the frame with wooden joists results in semi-rigid behaviour, indicating the in-plane stiffness is largely attributed to the wood floor. (Li, He, Guo, & Ni, 2010) In keeping with the I-beam analogy, the equation for in-plane deflection of hybrid timber-steel joisted floors can be adapted from the all-wood equation [7] in two different ways based on two separate assumptions. The first assumption is to treat the wood floor to be perfectly connected to the steel frame resulting in ideal I-beam behaviour. This method assumes that complete shear transfer is achieved through joist hangers and bolted ledger, resulting in axially stressed steel chords. Under this assumption the fourth term, chord splice slip, can be neglected since steel members can be fabricated to suit whatever span is required, and the first term capturing flexural deflection can be used by inputting values for the steel chord section rather than a wood chord section. This assumption leads to the following modified version of [7]:

$$\Delta_d = \frac{5vL^3}{96EAL_D} + \frac{vL}{4B_v} + 0.000614Le_n \qquad [9]$$

A less conservative, though not unjustified, approach could lead to the elimination of the flexural term altogether, since as shown in Figure 24, flexural deflections for most practical applications do not have a significant impact on global diaphragm behaviour, the substitution then of a material with 18 times greater elastic modulus and similar cross-sectional area leads to virtually no flexural contributions to diaphragm deflection, resulting in the following, unconservative modification of [7]:

$$\Delta_d = \frac{vL}{4B_v} + 0.000614Le_n \qquad [10]$$

The behaviour described in the previous equations is not unrealistic when considering that joist hangers are considered capable of providing full shear transfer into sawn lumber chords, reflected by the design deflection equation where chords are considered to be only stressed in compression or tension. The only unknown assumption then is considering the shear transfer provided by the web-bolted ledger into the steel beam. With appropriate bolt spacing, this should not be considered unreasonable. When estimating diaphragm deflection in this manner, care should be taken to ensure bolted ledgers and joist hangers can provide sufficient shear transfer into the steel chords to develop axial stress and that this shear transfer does not result in splitting of the wooden ledger.

The second method is based on the assumption that shear transfer between joist hangers and ledger, and between ledger and steel beam, is insufficient to develop axial stress in the steel chords. Under this assumption, joisted construction within a steel perimeter frame is seen to behave in the same manner as exclusively wood joisted floors. The justification for this approach is made by considering the integrity of the ledger-bolt connection. When stressed in shear the connection is likely to experience initial slip before contacting the edge of the bolt hole in both the ledger and web. Once the slip is recovered the developing shear stress may cause bearing and possibly splitting failure in the ledger, in this event the ability of the steel beams to develop axial stress is completely negated. Where this diaphragm behaviour the influence of the chords should be disregarded, meaning end panels must resist bending stresses in addition to shear stresses as shown in (Bott, 2005).

Ultimately the influence of the steel chords is limited to the flexural behaviour of the diaphragm and is not as impactful on global diaphragm stiffness as the shear properties are. The true behaviour of the ledger-web shear transfer is dependent on framing details and requires experimental investigation. In lieu of data and any relevant design code provisions, the method in [9] and [10] is recommended for assessing the in-plane behaviour of timber-steel hybrid diaphragms.

The in-plane behaviour of panel floors on perimeter steel framing can be considered similar to the behaviour of wood-only construction. As previously mentioned, most panel floors are rigid in-plane and the addition of steel perimeter beams is unlikely to significantly alter this behaviour. Of greater importance is the behaviour of panel-panel spline connections. The rigid assumption was made in the Scotia Place structure where glulam planks were connected on top of steel I-beam sections and plank bending behaviour, disregarding the influence of the steel, was assumed. (Moore, 2000)

4.2 Finite Element Modelling

This portion of the thesis uses finite element modeling using commercially available structural analysis program SAP2000 to investigate the effects of infilled wood-joisted diaphragms in steel construction.

4.2.1 Introduction

Finite element models were constructed in SAP2000 to investigate the impact of joisted wood diaphragms on concentrically-braced steel frame structures under seismic loading. Three-dimensional models of varying height, layout and stiffness were created following the simplified analysis method presented by Li et al. and were assessed using a linear dynamic method analysis method known as response spectrum analysis. The modeling is focused on assessing the impact of lightweight diaphragms on global structural response by varying building height, plan aspect ratio, and ratio of diaphragm to frame stiffness. In addition, force results based on capacity design principles will be compared with code-listed shear strength values to determine the feasibility of wood-based floors in braced frame construction. A design-oriented approach towards the finite element modeling is taken by using a simplified model and conducting linear dynamic analysis rather than a detailed structural model and applying more advanced non-linear dynamic analysis. As was demonstrated in the research by He et al., it has been shown that timber diaphragms in steel construction remain elastic during both elastic and inelastic phases of the steel frame, thereby validating the use of elastic analysis in this work. Further to this end, design and analysis in this section follows the requirements of non-yielding diaphragms on non-wood SFRS, as described in Clause 9.8.5.2.2 of CSA 086.

4.2.2 *Diaphragm Modeling*

The simplified approach to modeling wood diaphragm behaviour in hybrid frames discussed by He and Li is also used here. Linear 1-DOF diagonal braces have been shown to accurately represent the distribution of lateral forces between frames and also allow for simple hand analysis enabling the designer to adjust diaphragm-frame stiffness ratios quite easily. (Li, He, Guo, & Ni, 2010) (Ma & He, 2012) Specific experimental data is not used for determining diaphragm stiffness but rather CSA 086 guidelines for diaphragm deflection are used to provide a range of diaphragm/brace stiffness. Though experimental data provides the most accurate estimate of the properties of a specific design, testing is time-consuming, costly, and limited to a small range of design configurations. For research focused on design aspects of timber diaphragms, estimates from CSA 086, which are based on experimental data themselves, are seen to be adequate.

The stiffness of a diaphragm as a function of diagonal brace stiffness configured as seen in Figure 25 is determined by analysis of a simply supported 2D-diaphragm.

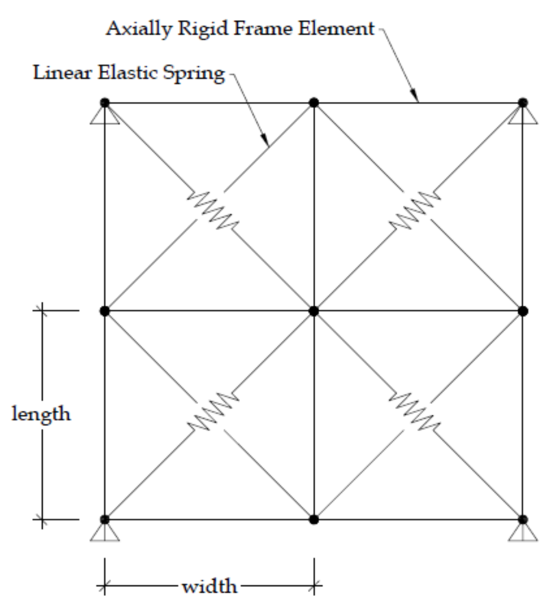

Figure 25: 2x2 bay diaphragm

The diaphragm stiffness is first determined by analysis of a single diagonal brace:

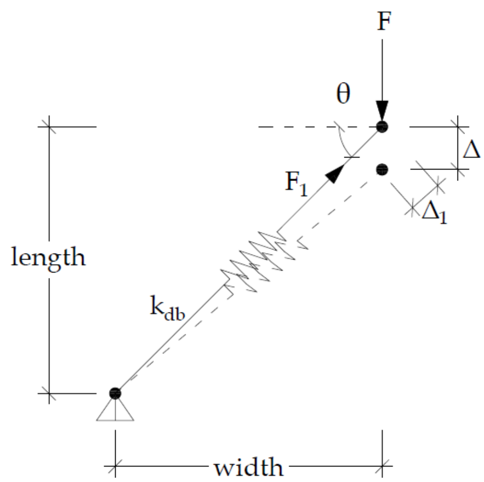

Figure 26: Stiffness of single linear brace (other elements not shown for clarity)

$$F_1 = \frac{F}{sin\theta}$$

$$u = \frac{u_1}{sin\theta}$$

$$F_1 = k_{db} \times u_1$$

$$\frac{F}{sin\theta} = k_{db} \times usin\theta$$

The stiffness of one 1-DOF brace, k_{db}, as a function of the global force, *F*, and global deflection, u, is then:

$$k_{db} = \frac{F}{u}\frac{1}{sin^2\theta} \quad [11]$$

The problem of determining overall diaphragm stiffness of a 2x2-bay diagonally braced floor, like the one shown in Figure 27 is simplified when considering the steel beams to be axially rigid and the floor force is considered to be a concentrated load at midpoint of the floor. The rigid assumption is valid considering the brace stiffness ranges between 0 – 5x10^3 N/mm, while the axial stiffness of 5000 mm-long W250x101 beam is 5.2x10^5 N/mm, making the ratio of brace-to-beam axial stiffness less than 1%. If all braces have equal stiffness the overall diaphragm stiffness becomes the sum individual braces.

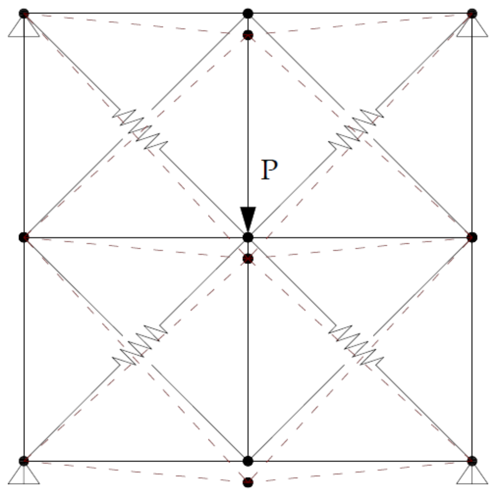

Figure 27: Braced diaphragm

The vertical component of the load per brace is $F = P/8$, which can be substituted into [11] to yield the individual brace deflection, u, which is also equal to the global diaphragm deflection, u_d, namely:

$$u_d = \frac{P}{8}\frac{1}{k_{db}}\frac{1}{sin^2\theta} \qquad [12]$$

The diaphragm stiffness, k_d, is governed by the equation

$$k_d = \frac{P}{u_d} \qquad [13]$$

Substituting [12] into [13], yields the diaphragm stiffness as a function of brace stiffness:

$$k_d = 8k_{db}sin^2\theta \qquad [14]$$

To determine the relative stiffness ratio the frame stiffness must also be determined. Two-bay frames on either end of the diaphragm transfer the load P from the diaphragm to the supports. Each frame consists of two bays and four diagonal braces. Steel column-beam connections are pinned so that the lateral load is taken exclusively by the diagonal braces.

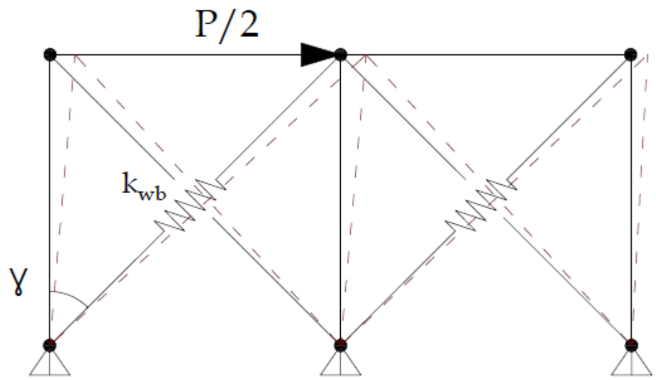

Figure 28: Braced frame

The scenario is analysed in the same fashion as the diaphragm. Two parallel frames (one on either side of the diaphragm), share the load *P*, and four braces resist *P/2* meaning frame deflection, u_f, and stiffness, k_f, as a function of wall brace stiffness, k_{wb}, are

$$u_f = \frac{P}{8}\frac{1}{k_{wb}}\frac{1}{sin^2\gamma} \quad [14]$$

$$k_f = 8k_{wb}sin^2\gamma \quad [15]$$

For the case of diaphragm-frame stiffness equal to unity, the deflection u_f and u_d are equated, yielding the following relationship between wall brace and diaphragm brace:

$$k_{wb} = k_{db}\frac{sin^2\theta}{sin^2\gamma} \quad [16]$$

[16] can be manipulated to yield the desired relative stiffness ratio.

Relative stiffness ratios, $r = k_d/k_f$ tested are r = 0.00, 0.25, 0.50, 0.75, 1.00, 1.50, 2.00. Where r = 0 represents the flexible condition, r = 0.75, 1.0 represent the semi-rigid condition and r = 2.0 represents the rigid condition. To determine required frame, diaphragm, diagonal frame brace and diagonal diaphragm brace stiffness for implementation into SAP2000, the required frame stiffness is determined first by limiting the 1st floor storey drift to 1.00% based on static equivalent loading. The frame diagonal frame brace can then be determined through [15], required diaphragm diagonal brace stiffness can be determined with [16] and applying the selected r-value, and the resulting diaphragm stiffness is determined through [14].

The relative stiffness ratio, r, between diaphragm, k_d, and frame, k_f, per storey is calculated through the following expression:

$$r = \frac{k_d}{k_f} \qquad [17]$$

Relative stiffness ratios are varied in the analysis to include values of r = 0.00, 0.25, 0.50, 0.75, 1.00, 1.50 and 2.00. Table 10 outlines the diaphragm classification based on relative stiffness ratio.

Table 10: Diaphragm classification

r	Diaphragm Classification
0.00-0.25	flexible
0.50-0.75	semi-rigid
1.00-2.00	rigid

4.2.3 Building

To mimic typical residential and commercial structures, models were constructed with three, six, and nine-storey heights, each tested at three separate plan aspect ratios of 1:1, 1:2, and 1:3, where the long direction is perpendicular to the direction of loading (x-direction). Each model is two bays deep, parallel to the load and four bays wide, perpendicular to the load (y-direction); the y-direction bays were kept at 5000 mm widths and x-direction bays at 2500 mm, 5000 mm, and 7500 mm with storey height consistently 3000 mm. The structure is a concentrically braced steel frame system with each building have both y-direction bays braced over the full height of the structure for all building configurations. The steel frame is comprised of W-shape beams and columns of varying size, depending on the building size. Beam ends are released from shear and bending while vertical columns are moment connected and pinned at the base. Generic steel tension-compression non-buckling braces are used.

In compliance with NBCC load combination provisions, the design gravity loads are multiplied and combined according to the appropriate limit states load factors and combinations. The seismic weight of the structure accounts for the full dead load and one quarter the roof snow load. Table 11 summarizes the design loads for both wood and concrete floor/roof options. Self-weight of steel superstructure is calculated by the program.

Table 11: Design Loads Summary

Engineered Joist Floor			
Roof Load (kPa)			Floor Load (kPa)
Live load	1.90	1.90	Live load
Roofing	0.18	0.30	1/2" drywall
Insulation	0.02	0.10	Spanning member
5/8" sheathing	0.08	0.20	Ceiling + strapping
Spanning member	0.10	0.20	Services
Mechanical	0.20	1.00	1" topping & finishes
Ceiling	0.10	0.50	Partitions
Snow	1.82	-	-
Factored gravity load (kPa)	*4.61*	*5.74*	*Factored gravity load (kPa)*
Factored seismic weight/area (kPa)	*1.14*	*2.31*	*Factored seismic weight/area (kPa)*

Steel framing elements were selected based on factored gravity loads from Table 11 while lateral brace stiffness design was based off of limiting storey deflection to roughly 1% when loaded with the static equivalent forces using the factored seismic load from Table 11, as mentioned previously. Plan and elevation views of the tested structure are shown in Figure 29.

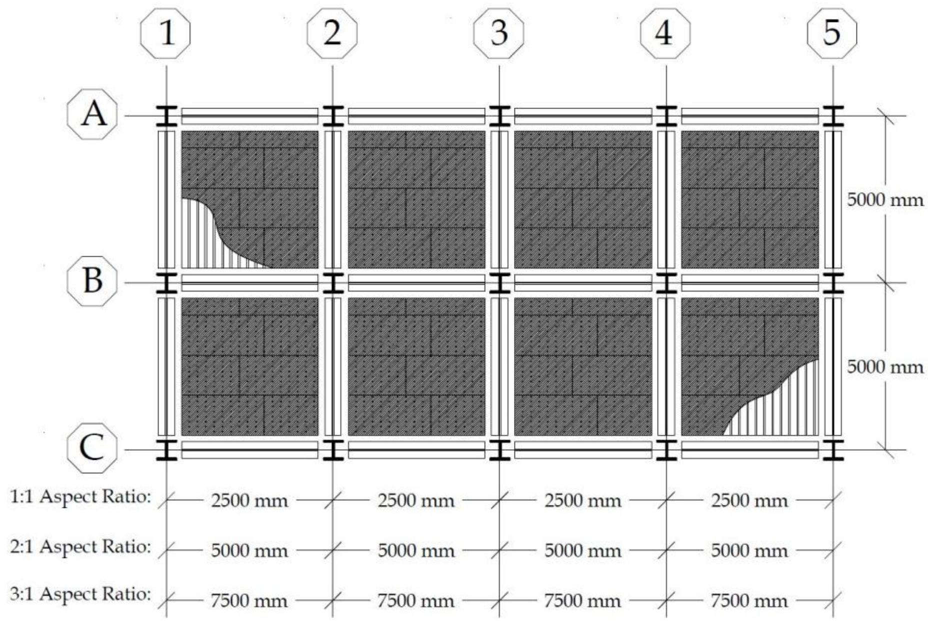

Figure 29: Plan view of building

4.2.4 SAP2000

The structural analysis program SAP2000 is used here in light of the design-oriented approach of this research; the program is made commercially available by the reputable structural software company Computers & Structures Inc. and is used in engineering offices worldwide. SAP2000 is known to be a "user-friendly" program featuring a versatile graphical interface, user-defined material and section options, and with linear, non-linear, static, and dynamic analysis capabilities. The program uses determines the stiffness matrix of the built model to implement in the finite element method to solve the governing differential equation.

4.2.5 Model

The structural model is created in SAP2000 using frame, link, and shell elements. Steel framing members are modeled as frame elements selected from the programs database of CISC shapes using 350W steel. As mentioned, storey columns are fully fixed to subsequent storeys allowing transfer of bending, shear, axial, and torsional forces while beams are pinned allowing for transfer of axial forces only. Link elements are used to model the diagonal bracing representing the diaphragm as well as the diagonal bracing of the braced bays. Link elements allow users to manually define stiffness properties for all six degrees of freedom (DOF) at each element end. The two-joint links used here have one degree of freedom, translation along the longitudinal axis, the stiffness of which is adjusted to represent an array of diaphragm, braced bay, and relative stiffnesses. Shell elements are used to supply a surface upon which the seismic masses may be applied and are not considered to add any lateral stiffness to the structures. Shells are connected to frame elements at the four corner locations and since they are not meshed the load is transferred directly to the node points. Though this technique results in beams that are not directly stressed since they are not involved in the load path between floor and column, beam demand and sizing is not a central goal of this research and it is deemed that this will not have a significant influence on the global structural behaviour and is determined to be acceptable. The factored seismic weight per area from Table 11 was applied as a mass to the shell elements in the model. A summary of designed elements and their analytical representations is shown in Table 12.

Table 12: Model components

Component	Structural Member	Model Element	Properties
Columns	W250x101 W350x97	frame	E = 200 000 MPa
Beams	W250x24 W250x101	frame	E = 200 000 MPa
Bracing	tension-compression only HSS	link	K_1 = 4500-6000 N/mm $K_2 = K_3 = 0$
Diaphragm	sheathed joists	link	K_1 = 0 - 20000 N/mm $K_2 = K_3 = 0$
Area surface		shell	$E_1 = E_2 = E_3 = G = 0$

4.2.6 Response Spectrum

Response spectrum analysis is a linear dynamic analysis method commonly used in industry and implemented in most codes and standards as a more comprehensive model compared to static equivalent force methods. The response spectrum depicts the relationship between period and acceleration based on location specific seismology. The NBCC provides spectral accelerations for periods of 0.2s, 0.5s, 1.0s, 2.0s, and recently 4.0-10.0s, for every urban centre countrywide. Most building structures have many vibrational modes each with their own period and the structure may be excited in any single mode or combination of modes during a seismic event. The response spectrum calculates the anticipated accelerations for each mode and combines them using one of several methods, most capable of which is the complete quadratic combination (CQC).

The response spectrum used in this analysis is for Vancouver (Granville & 41^{st}), the site class category "C". The spectral accelerations are listed in Table 13. SAP2000 allows users to define the input response spectrum multiplied by the appropriate scaling factor to achieve the desired acceleration, in this case the factor is taken as the gravitational constant, *g*. Accelerations are applied only in one direction, parallel to the braced bays.

Table 13: Seismic data for Vancouver (Granville & 41^{st} Ave.)

$S_a(0.2)$	$S_a(0.5)$	$S_a(1.0)$	$S_a(2.0)$	PGA
0.95	0.65	0.34	0.17	0.47

4.2.7 Test Summary

Nine different structures are tested each with five different diaphragm-frame stiffness ratios. The stiffness ratios are estimated using [17] derived from statics earlier. A summary test matrix is provided in Table 14. Test names are explained as follows:

height - 3 storey   *diaphragm aspect ratio* - 2:1   *diaphragm-frame stiffness ratio* - 3:1

H3-A2-R3

Table 14: Linear dynamic analysis test matrix

	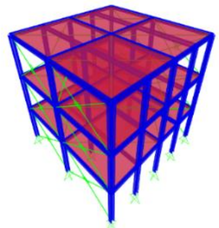	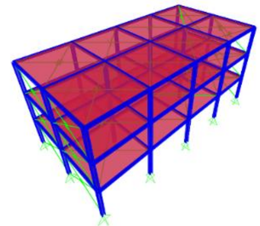	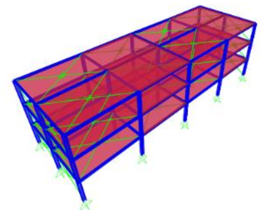
Storeys	3	3	3
Aspect Ratio	1:1	1:2	1:3
Relative Stiffness Ratio	0, 0.25, 0.50, 0.75, 1.0, 1.5, 2.0	0, 0.25, 0.50, 0.75, 1.0, 1.5, 2.0	0, 0.25, 0.50, 0.75, 1.0, 1.5, 2.0
Test Names	H3-A1-R0 → H3-A1-R2	H3-A2-R0 → H3-A2-R2	H3-A3-R0 → H3-A2-R2
	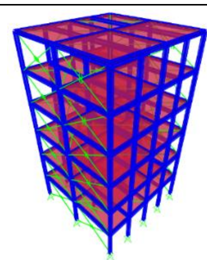	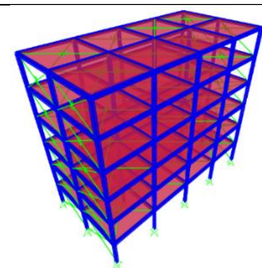	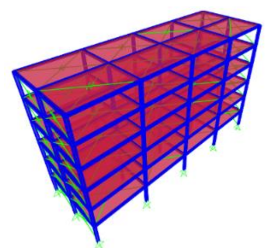
Storeys	6	6	6
Aspect Ratio	1:1	1:2	1:3
Relative Stiffness Ratio	0, 0.25, 0.50, 0.75, 1.0, 1.5, 2.0	0, 0.25, 0.50, 0.75, 1.0, 1.5, 2.0	0, 0.25, 0.50, 0.75, 1.0, 1.5, 2.0
Test Names	H6-A1-R0 → H6-A1-R2	H6-A2-R0 → H6-A2-R2	H6-A3-R0 → H6-A3-R2
	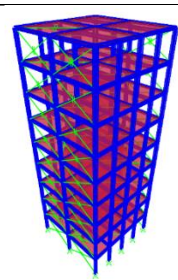	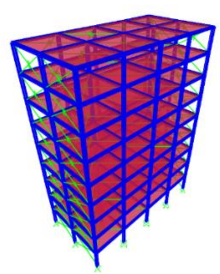	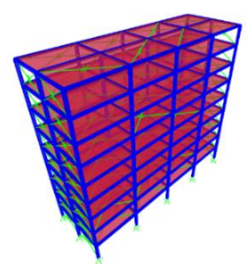
Storeys	9	9	9
Aspect Ratio	1:1	1:2	1:3
Relative Stiffness Ratio	0, 0.25, 0.50, 0.75, 1.0, 1.5, 2.0	0, 0.25, 0.50, 0.75, 1.0, 1.5, 2.0	0, 0.25, 0.50, 0.75, 1.0, 1.5, 2.0
Test Names	H9-A1-R0 → H9-A1-R2	H9-A2-R0 → H9-A2-R2	H9-A3-R0 → H9-A3-R2

4.2.8 *Results*

The finite element model is used to examine several parameters of hybrid timber-steel structures. The impact on diaphragm forces resulting from varying relative stiffness ratios and aspect ratios is investigated, the ability of joisted wood floors to achieve relative stiffness ratios based on CSA 086 allowances is assessed, and diaphragm shear demands are compared with diaphragm strength values provided in CSA 086 in light of capacity design principles for non-yielding diaphragms on non-wood SFRS.

Diaphragm demands are discussed in terms of forces calculated in the finite element models. Clause 9.8.5.5.2 of CSA 086 dictates that design diaphragm forces, V_{Di}, for wood-based diaphragms supported on non-wood SFRS are to be calculated as such:

$$V_{D_i} = \gamma_i F_i \quad [18]$$

Where the lateral storey force, F_i, based on force modification factors $R_D R_O$ for the SFRS, is multiplied by the storey overstrength coefficient, γ_i, according to capacity design principles. Force modification factor R_D as provided by the NBCC is 3.0 for moderately ductile concentrically braced steel frames and 2.0 for limited ductility concentrically braced steel frames. Both force modification factors will be used in this analysis. The overstrength factor R_O for both is given as 1.3. The storey overstrength coefficient is dependent on the design of the SFRS. Since the analysis is linear elastic and the SFRS consists of linear elastic braces, calculating an overstrength coefficient is arbitrary. The storey overstrength coefficient used in this analysis is 1.25. It is important to note the difference between the diaphragm design force based on non-wood SFRS vs. wood-based SFRS. CSA 086 states the diaphragm shear demand in wood-based SFRS structures is taken as the seismic storey force (same as for non-wood SFRS) multiplied by the overstrength coefficient, to a maximum multiplier of 1.2. Whereas in steel construction this value can be greater than 1.2, indicating design forces for wood diaphragms on non-wood SFRS may be higher than on wood-based SFRS. In summary, the diaphragm forces presented forthwith represent the storey force as calculated by the computer program divided by force modification factors $R_D R_O$ and multiplied by overstrength coefficient 1.25, and do not represent actual force values from the diaphragm itself.

4.2.8.1 Relative Stiffness Ratio and Aspect Ratio

Figure 30,Figure 31, and Figure 32 depict the variation in diaphragm design shear, V_D, for the listed stiffness ratios as described in Table 10.

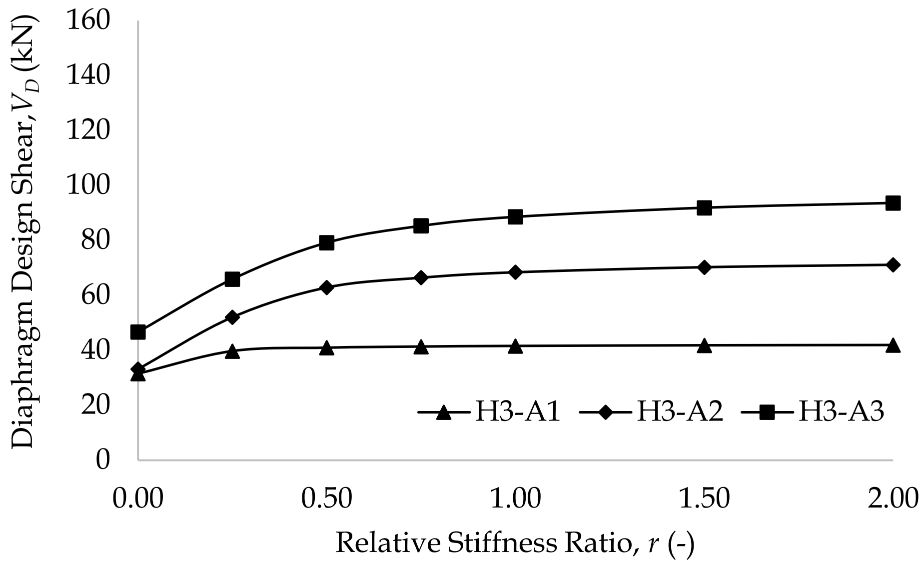

Figure 30: Diaphragm design shear vs. relative stiffness ratio for 3-storey height

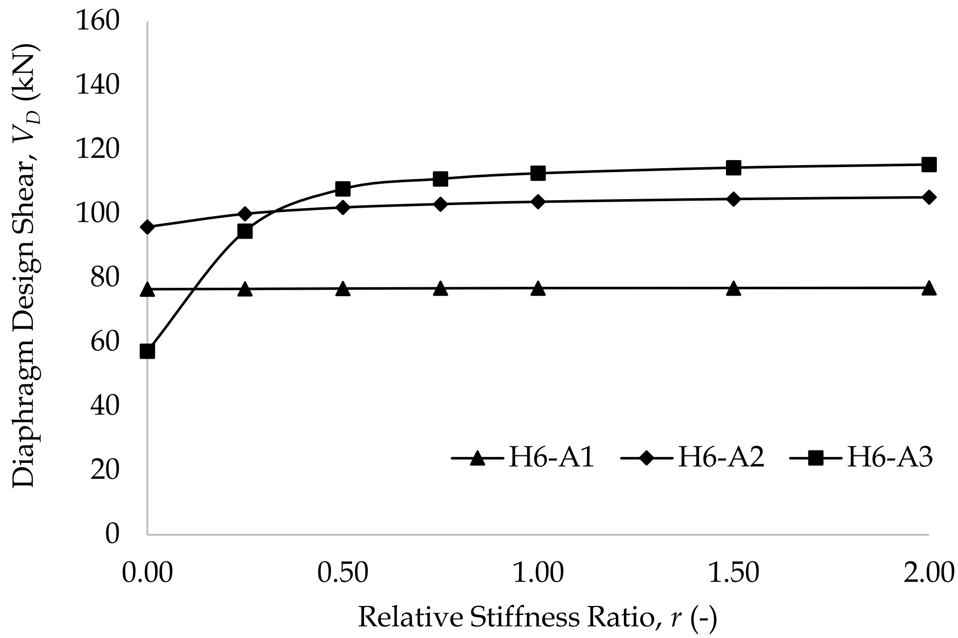

Figure 31: Diaphragm design shear vs. relative stiffness ratio for 6-storey height

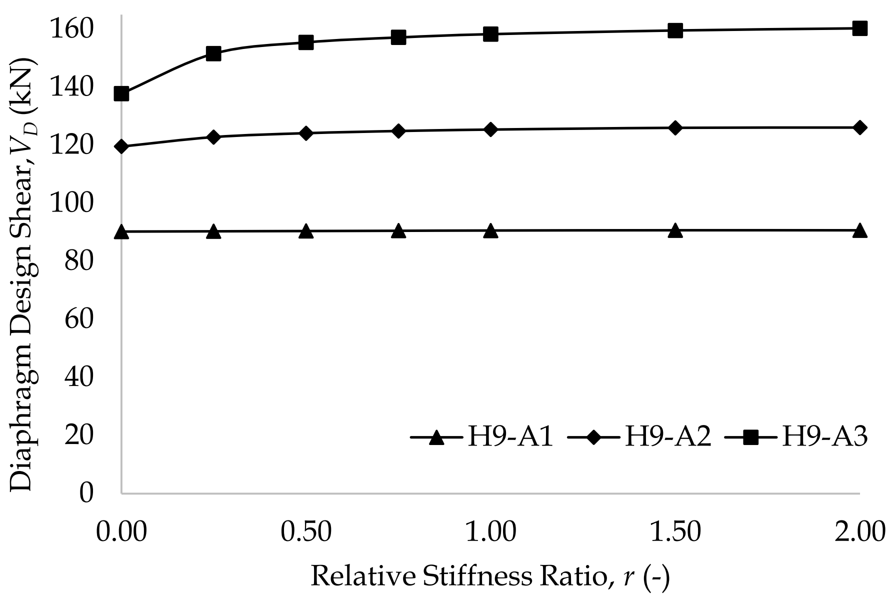

Figure 32: Diaphragm design shear vs. relative stiffness ratio for 9-storey height

Figure 30, Figure 31, and Figure 32 demonstrate the influence on diaphragm design shears, V_D, associated with increasing diaphragm stiffness relative to storey frame stiffness, *r*. The 3-storey structure shows significant increase in forces for values of *r* between 0 and 1, while the 6-storey structure demonstrates changes for *r* between 0-0.5, and the 9-storey structure shows impact simply over *r* values up to 0.25. Stiffening of the diaphragm (i.e. increasing *r*) results in some measure of overall structural stiffening which in turn reduces building period and increases accelerations of the structural mass, resulting in larger forces, hence the result is to be expected. While increasing diaphragm stiffness from the flexible condition, $r = 0$, to a rigid condition, $r = 1$, causes noticeable changes in diaphragm forces, increasing *r* beyond 1.0 yields virtually negligible results as seen in all three building heights.

Figure 30, Figure 31, and Figure 32 also illustrate the difference in diaphragm response to changing *r* with differing aspect ratios, *a*. Figure 30 shows relatively similar response to increasing *r* over all aspect ratios of the 3-storey structures. This behavioural similarity is a common result for short period structures where mass participation is predominantly first mode. The 6-storey structure shows differences in response between the first two aspect ratios (A1, A2) and the third (A3). The increase in diaphragm forces over the flexible - semi-rigid range is virtually negligible for A1 and A2, while A3 shows large increase in force from $r = 0$ to $r = 0.75$. H9 shows a similar trend to H6 in that A1 and A2 are unaffected by changing *r* while A3 once again experiences increasing force between $r = 0$ to $r = 0.75$. When observing the three results for A1 (H3-A1, H6-A1, H9-A1), it can be seen that with increasing storey height the influence of *r* begins to diminish to the point where in H6 and H9 there is virtually no evidence of *r* having an impact whatsoever. This trend is observed in A2 and A3 as well, where increasing storey height has a “flattening out” effect on diaphragm forces over the range of *r* values. A3 in particular demonstrates this result where the influence of *r* in H3 is significant up to $r = 1$, in H6 the impact extends to $r = 0.75$, and in H9 relative stiffness ratio creates differences in force only up to 0.25. This result indicates that diaphragm stiffness has a diminishing impact on global structural stiffness as storey height increases.

Though the observation that increasing diaphragm stiffness does not increase diaphragm forces (H6-A1, H9-A1) seems to contradict basic force-deformation relationship, it in fact does not. Firstly, the results for diaphragm force are not taken from the diaphragms themselves, but rather through capacity design principles the forces are taken as a multiple of vertical brace load, as previously explained. However the same relationship would be seen where results were taken directly from diaphragms. Whereas increasing the stiffness of a vertical component theoretically attracts more lateral force into this component, this is not the case with diaphragms since the floor represents the only load path through which seismic weight can be transferred from the floor to the SFRS. In other words the diaphragm shear demand is not affected by diaphragm stiffness, aside from the increases in overall structural stiffness leading to larger structural accelerations.

It is also noted from Figure 30, Figure 31, and Figure 32 for each building height larger aspect ratios result in larger diaphragm forces, as summarized in Figure 33. These results are to be expected since all aspect ratios are varied with the same relative stiffness, hence increasing a only serves to increase structural mass.

It should be remembered that the aforementioned force results are not taken from the diaphragms but rather reflect the loads in the SFRS multiplied by the appropriate capacity design factors. As a result the discussed observations on the influences of changing relative stiffness and aspect ratio describe influences on global structural response, and not on diaphragm response.

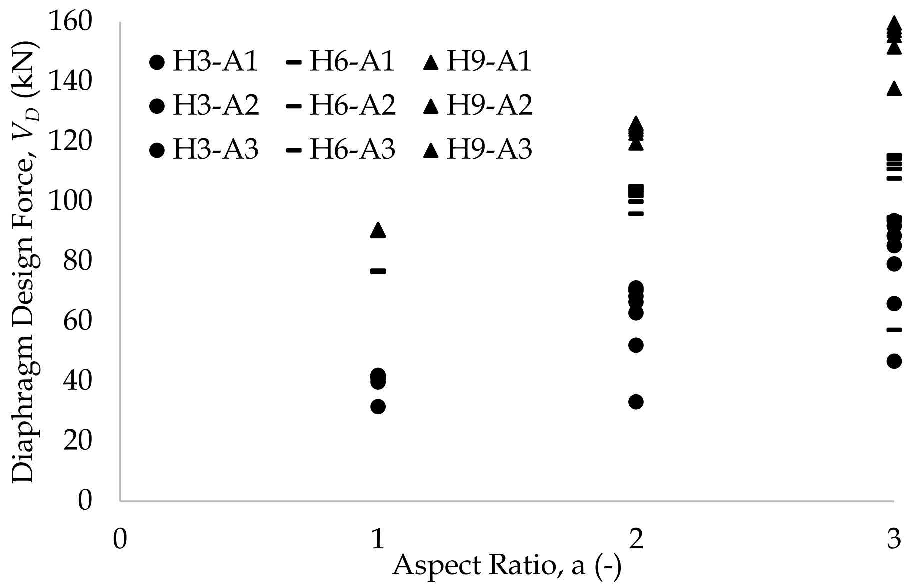

Figure 33: Diaphragm design force vs. aspect ratio for all building heights

Plots of diaphragm design force vs. relative stiffness showed that results do not significantly increase beyond r = 1.0, that larger aspect ratios are more affected by relative stiffness ratios, and that influence of r decreases with increasing building height.

The plots of design force vs. relative stiffness do not reflect the response of diaphragms, but rather of the SFRS since demands are taken from the vertical bracing and multiplied by the capacity design factor to produce the design force. To investigate the response at the diaphragm level, plots of diaphragm deflection vs. relative stiffness are summarized in Figure 34, Figure 35, and Figure 36.

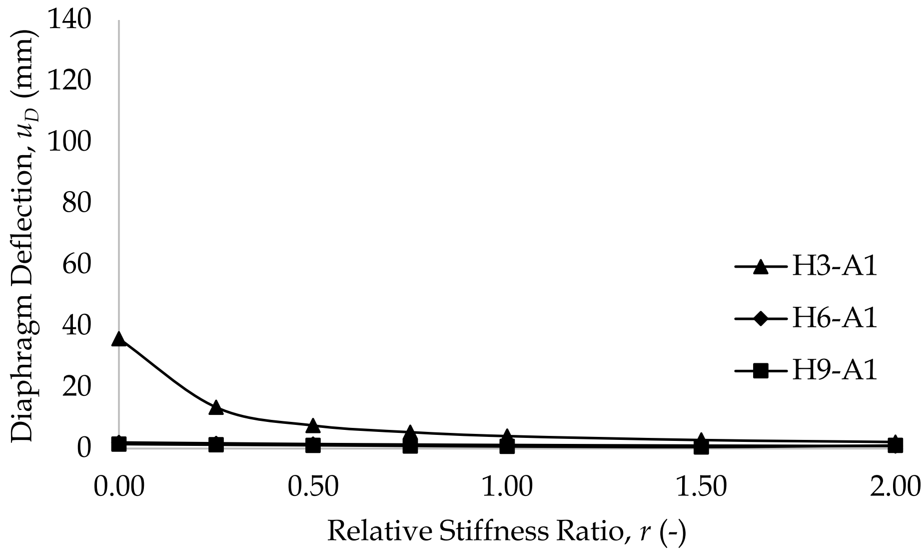

Figure 34: Diaphragm deflection vs. relative stiffness ratio, 1:1 aspect ratio

Figure 34 shows the relatively minimal impact in diaphragm demand as a function of relative stiffness. H3 does experience changes in demand from r = 0 to r = 1.0 while H6 and H9 show virtually no impact over the range of r values. These results are further evidenced by Table 15 where the ratio of deflections from the flexible condition (r = 0) to the semi-rigid condition (r = 0.75) and the ratio of deflection over the range of rigid conditions (r = 1.0, 2.0) are shown for all A1 structures. Both ratios describe the diaphragms dependence on increasing relative stiffness ratio. The average ratio of $u_{R0}/u_{R0.75}$ for 1:1 aspect ratio is 3.3 while the average ratio of u_{R1} / u_{R2} is 1.3. By comparison the same ratio using shear forces ($V_{D\text{-}R1}$ / $V_{D\text{-}R2}$) for A1 structures is at maximum 1.02.

Table 15: Change in diaphragm deflection due to r *for 1:1 aspect ratio*

Ratios of deflection (-)		u_{R0} / $u_{R0.75}$	u_{R1} / u_{R2}
A1	H3	6.72	1.90
	H6	1.53	1.43
	H9	1.66	0.68

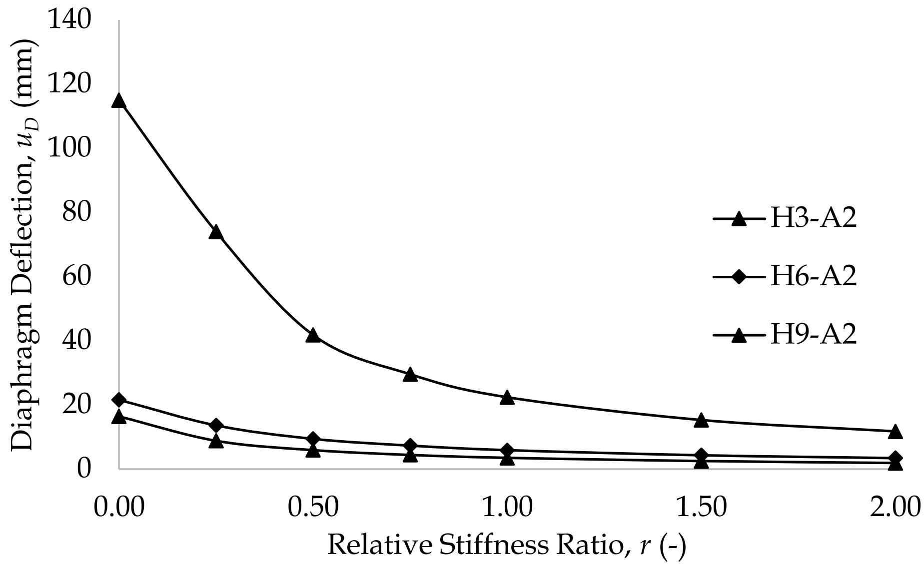

Figure 35: Diaphragm deflection vs. relative stiffness ratio, 2:1 aspect ratio

Figure 35 and Table 16 show more sensitivity to increasing relative stiffness ratios for H6 and H9 than seen for A1. The behaviour of H3-A2 is similar to that seen with H3-A1, though with a slightly less exaggerated ratio of flexible – semi-rigid deflection ratio. The average deflection ratio for a = 2 from Table 16 is 3.7, 12% greater than the value for a = 1, demonstrated greater vulnerability over the range of r values. A2 structures show slightly more influence from changing r than seen in A1 structures, with an average of 1.8, 30% higher than the A1 average. The maximum ratio $V_{D\text{-}R1}$ / $V_{D\text{-}R2}$ for A2 structures is 1.03.

Table 16: Change in diaphragm deflection due to r *for 2:1 aspect ratio*

Ratio of deflection (-)		u_{R0} / $u_{R0.75}$	u_{R1} / u_{R2}
A2	H3	3.89	1.90
	H6	3.57	1.73
	H9	3.73	1.73

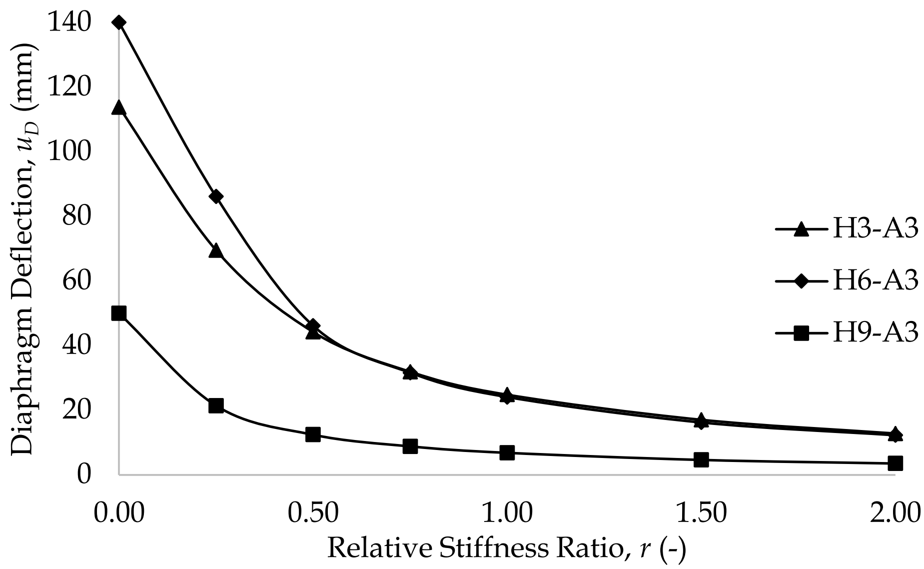

Figure 36: Diaphragm deflection vs. relative stiffness ratio, 3:1 aspect ratio

Figure 36 shows the greatest impact of changing stiffness of all three aspect ratios. The average ratio of $u_{R0}/u_{R0.75}$ for 3:1 aspect ratio is 4.6, 39% larger than A1 and 24% larger than A2, indicating diaphragm demands increase with increasing aspect ratio. In addition, the ratio of u_{R1} to u_{R2} is highest for 3:1 aspect ratio structures with an average of 1.95, 8% larger than A2, and 50% higher than the A1 average. The largest $V_{D\text{-}R1}$ / $V_{D\text{-}R2}$ ratio for A3 structures is 1.06.

Table 17: Change in diaphragm deflection due to r *for 3:1 aspect ratio*

Ratio of deflection (-)		u_{R0} / $u_{R0.75}$	u_{R1} / u_{R2}
A3	H3	3.57	1.94
	H6	4.43	1.96
	H9	5.68	1.94

The results for diaphragm deflection as a function of relative stiffness ratio indicate that diaphragm deflection is most significantly affected by relative stiffness ratios between r = 0-1, and to a lesser extent for r > 1. In comparison to the design forces, diaphragm deflection has much more sensitivity to r-values beyond 1 (27% more for A1, 75% greater for A2, and 84% more for A3). The flattening out effect, where increasing storey height reduces the influence of r on design shear as seen in the plots of V_D vs. r, is not clearly reflected in plots of u_D vs. r. A3 structures display this effect conclusively, however the opposite is seen in H9 and results from H6 are ambiguous in this regard.

4.2.8.2 In-Plane Stiffness Requirements

As previously mentioned, frame stiffness is selected based on limiting 1st floor inter-storey drifts to 1.00% and diaphragm stiffness is determined based on the appropriate relative stiffness ratio, r, as opposed to inputting experimental results for diaphragm stiffness. To assess the feasibility of achieving these stiffness values, Clause 9.7.2 of CSA 086 is employed to determine the maximum achievable code-listed stiffness. The available stiffness is determined by manipulating [7], the diaphragm deflection under averaged shear load, v, to obtain the global diaphragm stiffness. Table 18 summarizes the available stiffness for varying designs compared to the required stiffness for all r values. Three separate frame stiffness are used, one for each building height.

Note that the global stiffness values in Table 18 don't change with nail spacing since nail deformation is similar for all cases as a result of the load per nail being greater than 1000 N in most cases (refer to Table A10.1 in CSA 086 for reference). Values in Table 18 are rounded to the nearest multiple of 0.25 for convenience.

Table 18: Achievable relative stiffness ratios for 1:1, 2:1, 3:1 aspect ratio

Plywood Thickness (mm)	Frame Stiffness (kN/mm)	Relative Stiffness Ratio $r = k_d\ /\ k_f$ (-)		
		A1	A2	A3
9.5	25	1.75	0.75	0.50
	30	1.50	0.75	0.50
	35	1.25	0.50	0.50
12.5	25	2.25	1.00	0.75
	30	1.75	1.00	0.50
	35	1.50	0.75	0.50
15.5	25	2.75	1.25	0.75
	30	2.25	1.00	0.75
	35	2.00	1.00	0.50
18.5	25	3.00	1.50	1.00
	30	2.50	1.25	0.75
	35	2.25	1.00	0.75

Table 18 summarizes the achievable relative stiffness ratios, r, for the three frame stiffness k_f = 25 kN/mm (3-storey), k_f = 30 kN/mm (6-storey), and k_f = 35 kN/mm (9-storey), based on code-listed estimations. As mentioned previously, a flexible diaphragm is assumed for r values between 0-0.25, a semi-rigid condition is assumed for r = 0.50-0.75, diaphragms with values of r greater than 1.0 are assumed to be rigid.

Table 18 demonstrates how 1:1 aspect ratios, regardless of floor design, can essentially always be considered rigid. The 9-storey 1:1 structure (H9-A1) can achieve rigid diaphragm behaviour with 9.5 mm plywood and the maximum allowable nail spacing (150 mm), however, as will be shown, though stiffness is easily achieved force demands may require larger dimension plywood to be used. The A2 column of Table 18 shows increasing difficulty in achieving rigid diaphragms. A minimum plywood thickness of 12.5 mm is required and the maximum achievable r is 1.5 using 18.5 mm ply, 9.5 mm ply can only achieve semi-rigid conditions. The rigid condition becomes increasingly unattainable with a 3:1 aspect ratio, where only a low frame stiffness (25 kN/mm) using the thickest ply, 18.5 mm, can achieve this condition. 9.5 mm, 12.5 mm, and 15.5 mm ply thicknesses are only capable of achieving semi-rigid conditions. The results from Table 18, in particular for A2 and A3, confirm the previously discussed conclusion that wooden joisted floors tend to behave as semi-rigid elements. (Huang, 2013)

Table 18 should be read in conjunction with Figure 7 which illustrates that for a 1-storey frame (correlating to the lowest frame stiffness in Table 18 – k_f = 25 kN/mm) r-values beyond ≈ 3.0 result in rigid diaphragms in terms of lateral load distribution.

4.2.8.3 Demand vs. Code Capacity

The diaphragm design forces are compared with code provided values for shear resistance of blocked and nailed wood-based diaphragms. Clause 9.5.2 from CSA 086 describes the shear resistance, V_{rs}, as follows:

$$V_{rs} = \phi v_d K_D K_{SF} J_{sp} L_D \qquad [19]$$

Where the performance factor ϕ is 0.7, the product $K_D K_{SF} J_{sp}$ is taken as unity, L_D is the diaphragm length in the direction parallel to the load, in metres, and the variable v_d represents the specified shear strength as found in Table 9.5.2. Specifed shear strength values are listed as a function of panel type, nail type and nail spacing. Nail spacings vary between 50-150 mm at diaphragm boundaries and 75-150 mm at other panel edges. A summary of specified strength values and global diaphragm stiffness for different plywood sizes and nail types and panel edge nail spacing for the diaphragm layouts shown in Figure 29 is shown in Table 19.

Table 19: Summary of diaphragm strength and stiffness

Plywood Thickness (mm)	Panel Edge Nail Spacing (mm)	Global Stiffness (kN/mm)			Shear Strength (kN)
		A1	A2	A3	
9.5	150	43.8	21.6	14.1	68.6
	100				102.9
	75				116.2
12.5	150	54.9	27.0	17.5	81.9
	100				123.9
	75				140.0
15.5	150	66.7	32.7	21.1	91.0
	100				137.2
	75				156.1
18.5	150	77.8	38.0	24.4	91.0
	100				137.2
	75				156.1

To illustrate the ability of wood-based diaphragms to achieve the capacity design strength requirements determined from the linear dynamic analysis performed in SAP2000, Figure 37-Figure 45 plot the available strength and stiffness of different diaphragm designs (using results from Table 19) against diaphragm design shear demands, V_D. Each figure includes demand values based on both R_D = 2.0 and R_D = 3.0, with each figure showing demand results for one aspect ratio. Each figure shows the available strength and stiffness capacity for each plywood thickness using the same panel edge nail spacing.

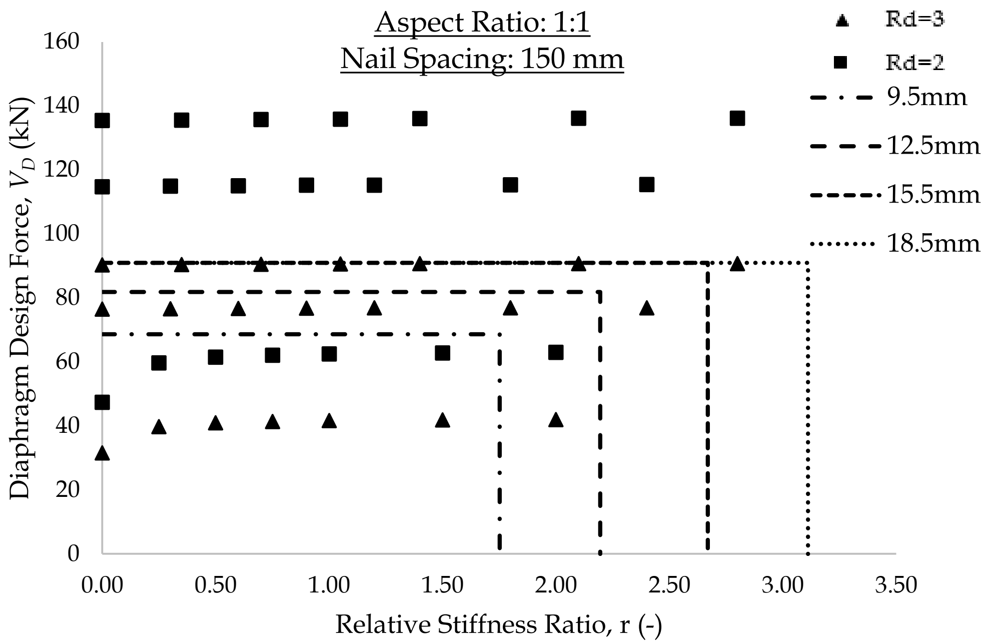

Figure 37: 1:1 aspect ratio diaphragm shear demand vs. plywood capacity - 150 mm nail spacing

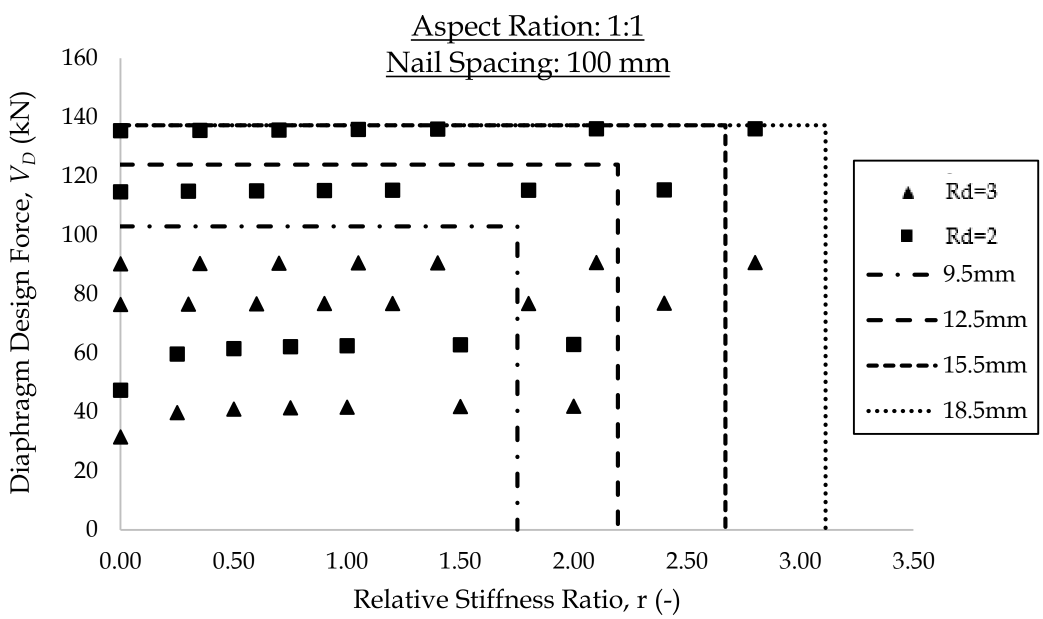

Figure 38: 1:1 aspect ratio diaphragm shear demand vs. plywood capacity - 100 mm nail spacing

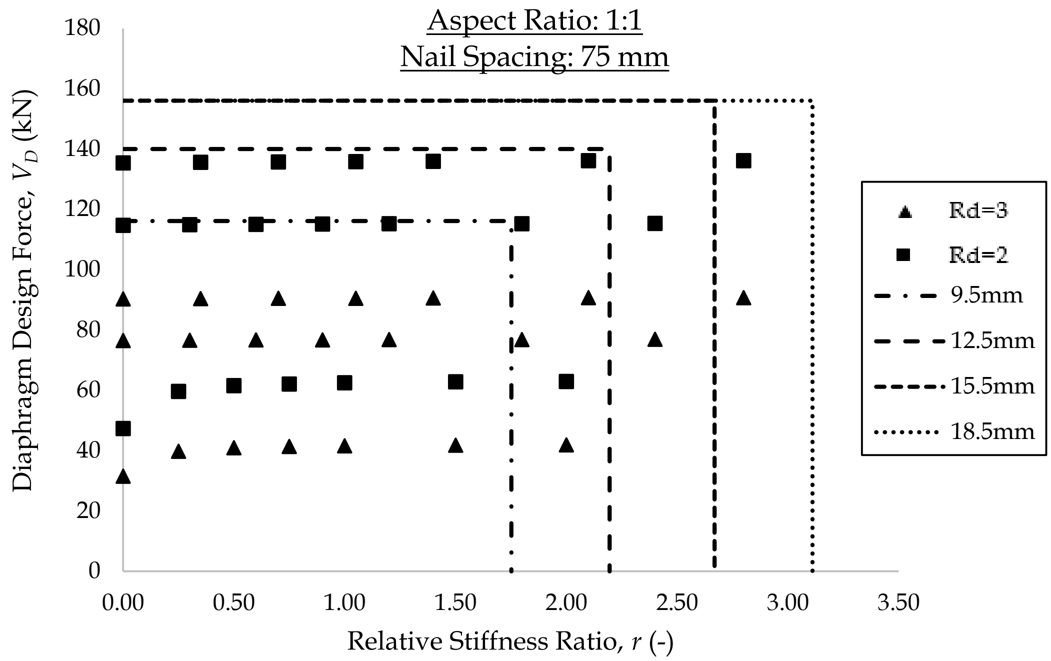

Figure 39: 1:1 aspect ratio diaphragm shear demand vs. plywood capacity - 75 mm nail spacing

Figure 37, Figure 38 and Figure 39 show the ability of plywood diaphragms of 1:1 aspect ratio to achieve strength and stiffness using 150, 100, and 75 mm panel edge nail spacing. Figure 37 clearly shows R_D values of 2.0 for H6 and H9 exceed diaphragm strength capacities. All other values of strength and stiffness are achievable using 18.5 mm plywood. By contrast 9.5 mm plywood is only suitable strength wise for H3 structures of R_D of 2.0 and 3.0. A tighter nail spacing of 100 mm shows marked improvement, where both 15.5 and 18.5 mm ply can achieve required strength values and mostly adequate stiffness for all building heights and ductility factors. 9.5 mm ply can now provide shear resistance for all building heights using R_D = 3 and up to H6 using R_D = 2, though it fails to satisfy the high end stiffness requirements (r > 1.75). Using 75 mm edge nail spacing allows all height and R_D strength demands to be achieved using 12.5 mm plywood while achieving excellent stiffness (r > 2.0).

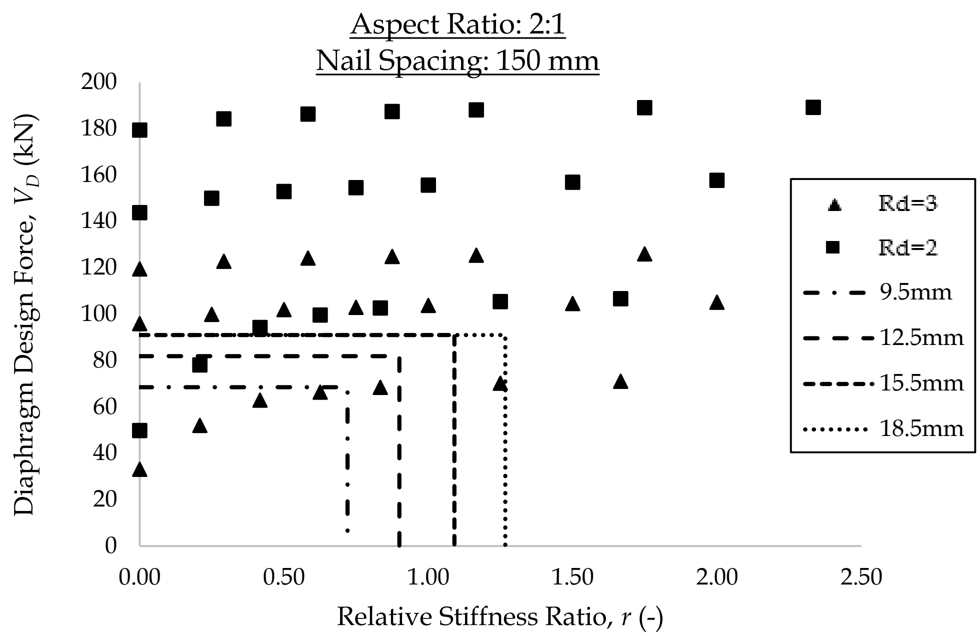

Figure 40: 2:1 aspect ratio diaphragm shear demand vs. plywood capacity - 150 mm nail spacing

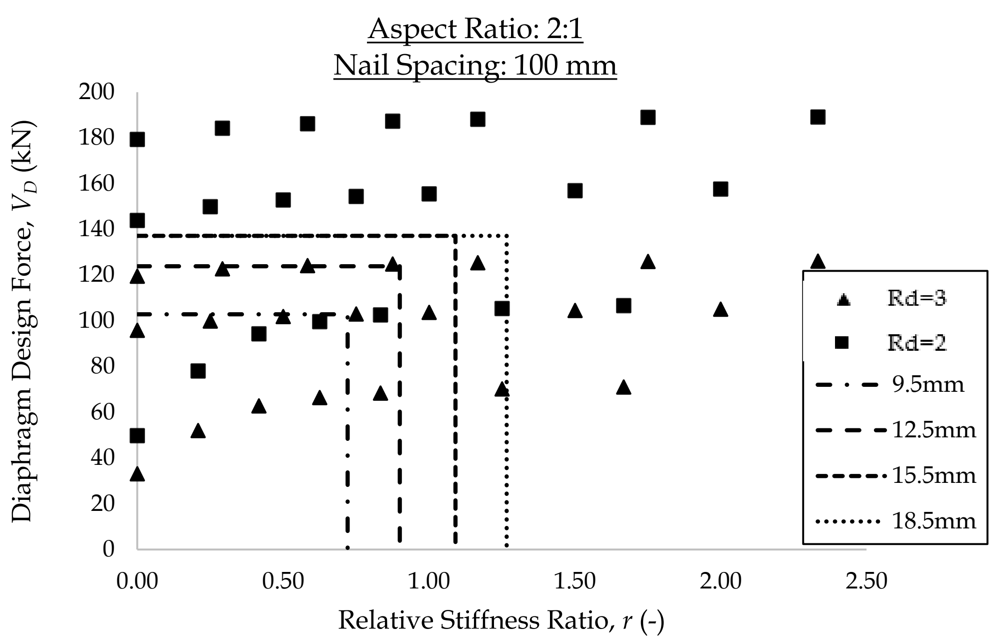

Figure 41: 2:1 aspect ratio diaphragm shear demand vs. plywood capacity - 100 mm nail spacing

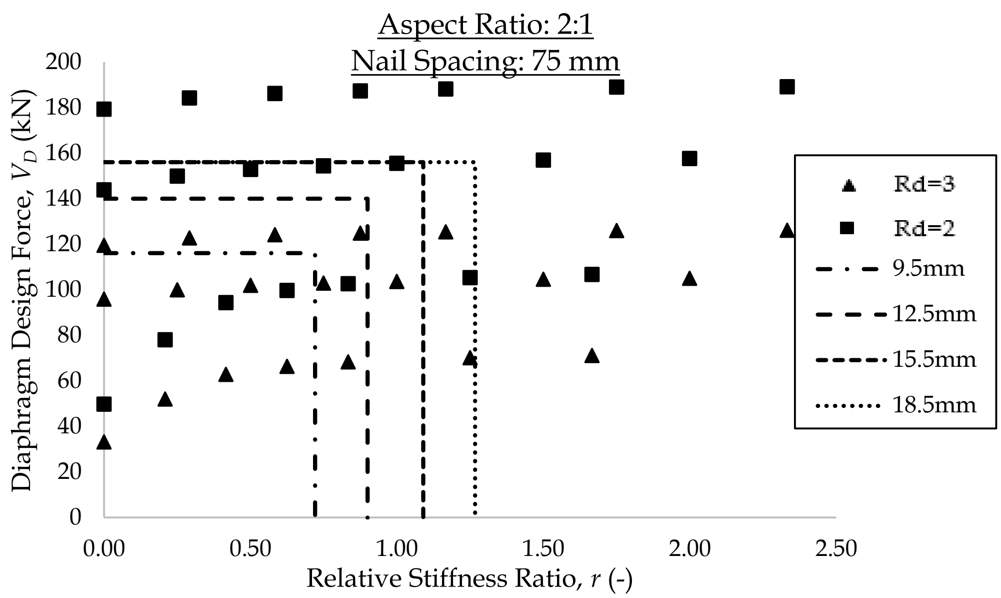

Figure 42: 2:1 aspect ratio diaphragm shear demand vs. plywood capacity - 75 mm nail spacing

Figure 40, Figure 41, and Figure 42 show the demand vs. capacity results for 2:1 aspect ratio floor plans. Diaphragm designs using 150 mm nail spacing hardly suffice with the increased aspect ratio. All plywood thickness are only capable of resisting H3 R_D = 3 strength demands while mostly providing semi-rigid stiffness. Again, the increase in force demands are to be expected for the larger aspect ratio, since the SFRS layout was not altered, hence the change in plan area results in larger forces going into the same amount of resisting elements creating larger capacity design demands for the diaphragm. Nail spacing of 100 mm allows shear demands to be covered by 9.5 mm for building height up to H6 using R_D = 3 and H3 using R_D = 2. With the same nail spacing (100 mm) 18.5 mm ply is capable of resisting shear demands for all R_D = 3 structures and for H3 R_D = 2 structures. As shown in Figure 42 the 75 mm nail spacing allows 15.5 and 18.5 mm ply to resist all demands save for H6 with R_D = 2. The 2:1 aspect ratio only allows diaphragm stiffnesses up to r = 1.25 (18.5 mm ply), whereas the taller structures (H6 and H9) have stiffness demands (k_f = 30, 35 kN/mm) exceeding what is achievable using code values.

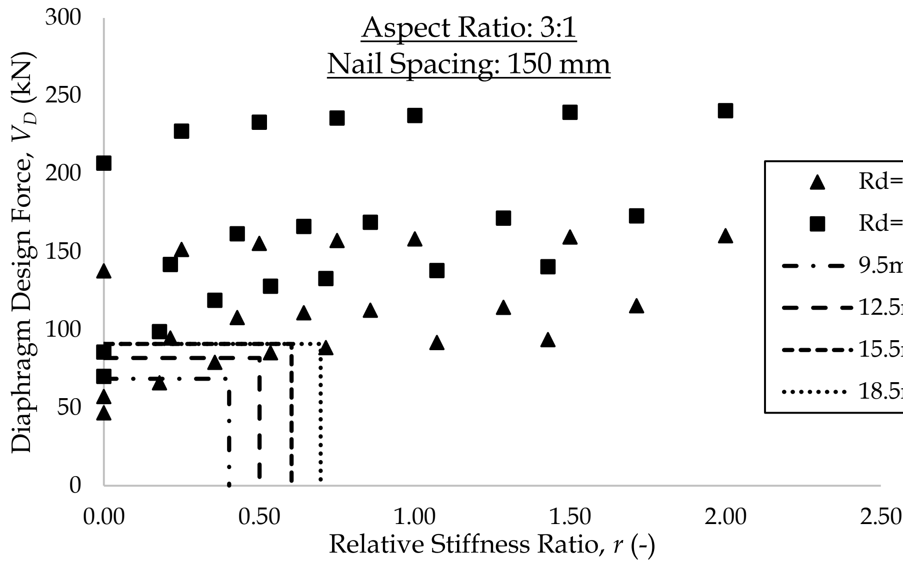

Figure 43: 3:1 aspect ratio diaphragm shear demand vs. plywood capacity - 150 mm nail spacing

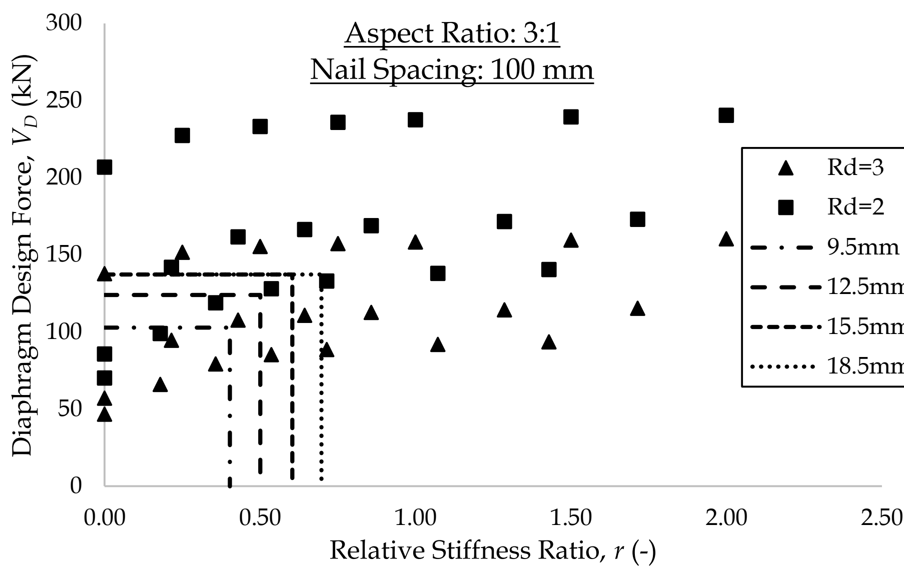

Figure 44: 3:1 aspect ratio diaphragm shear demand vs. plywood capacity - 100 mm nail spacing

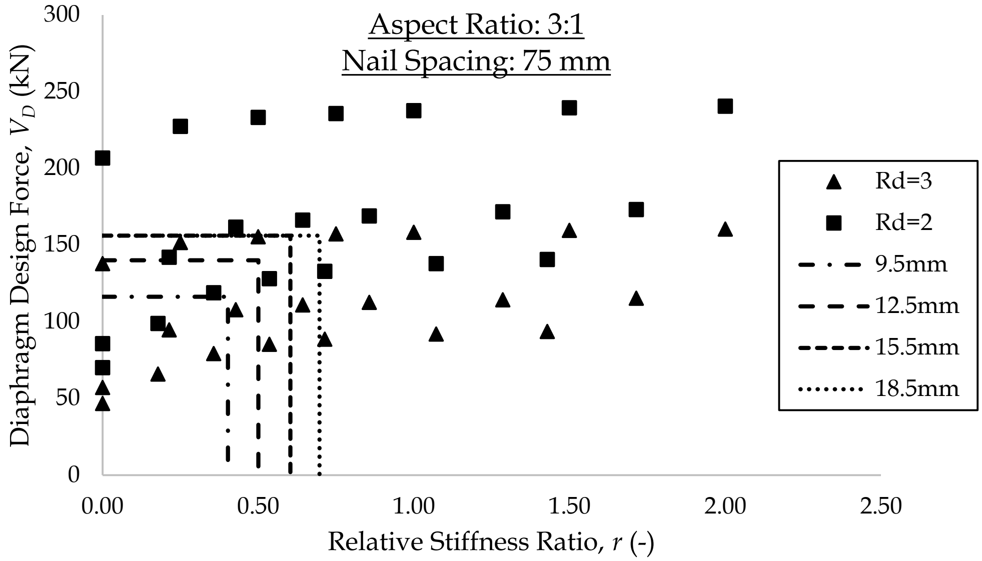

Figure 45: 3:1 aspect ratio diaphragm shear demand vs. plywood capacity - 75 mm nail spacing

Increasing the building dimensions further to a 3:1 aspect ratio results in higher force demands and difficult stiffness requirements, either of which the plywood diaphragms have a difficult time achieving. The 150 mm nail spacing design only allows the 15.5 mm and 18.5 mm ply to achieve enough strength for the lowest demands (H3, R_D = 3) at roughly 94 kN. Using a 100 mm nail spacing allows 15.5 and 18.5 mm ply to achieve strengths of 137 kN making H6 R_D = 3 and H3 R_D = 3 demands achievable. Even with a 75 mm spacing both 15.5 and 18.5 mm plywood fall short of achieving the required shear strength for H6 R_D = 2, and H9 R_D = 2 is far beyond capacity at over 200 kN. The range of stiffness for 9.5 mm to 18.5 mm plywood at the 3:1 aspect ratio lies between r = 0.4-0.7 while stiffness demands extend well beyond r = 1.5.

4.2.9 Conclusions

The finite element modeling of several different braced steel frame building configurations using diagonal bracing to represent wood-based diaphragm behaviour was conducted using linear dynamic analysis to assess the feasibility of wood-based floors in steel construction from a strength perspective based on capacity design principles. Building height, plan aspect ratio and diaphragm-frame stiffness ratio were varied and their respective influences assessed. Diaphragm strength demands and stiffness requirements were compared with shear strength and in-plane stiffness capacities as listed in CSA 086.

The influence of relative stiffness ratio, *r*, on diaphragm demand was investigated by varying diaphragm stiffness over a range of flexible, semi-rigid, and rigid conditions; the diaphragm demand is expressed as a multiple (1.25) of the maximum brace shear to represent the capacity design demand, not the actual diaphragm load. The relative stiffness ratio is found to influence shear demand up to r = 0.75-1.0, increasing stiffness ratios beyond this point are seen to have negligible impact. It is also observed that the influence of relative stiffness decreases with increasing building height, indicating global structural stiffness is less impacted by changes to diaphragm stiffness the taller the structure. The opposite affect is noted when increasing aspect ratio (between 1:1, 2:1, and 3:1), structures show an increased sensitivity to relative stiffness. Taller structures with lower aspect ratios display minimal dependence on relative stiffness. From a diaphragm level plots of diaphragm deflection vs. relative stiffness show a more exaggerated relationship with increasing r even for values beyond $r = 1$ than what is seen in force vs. r plots.

The feasibility of achieving semi-rigid and rigid diaphragm behaviour for 3, 6 and 9 storey structures with wood-based diaphragms was calculated based on a modified code estimations of diaphragm stiffness. The frame stiffness used in the analysis were based on limiting inter-storey drift at the base to 1%, resulting in 3 storey frame stiffness of 25 kN/mm, 6-storey frame stiffness of 30 kN/mm, and 9-storey frame stiffness of 35 kN/mm and diaphragm stiffness was based on a range of six values relative to the frame stiffness representing flexible, semi-rigid and rigid conditions. It was shown that wooden joisted diaphragms with 1:1 aspect ratios could achieve fully rigid behaviour while for aspect ratios of 2:1 most designs would yield a semi-rigid condition and increasing aspect ratio further to 3:1 resulted in only the strictest of design achieving semi-rigid behaviour. This is in agreement with reviewed experimental work demonstrating timber diaphragms mostly behave as semi-rigid members.

The feasibility of achieving capacity design shear demands at the base floor were assessed based on the strength allowances in CSA 086. Strengths were calculated for 9.5 mm, 12.5 mm, 15.5 mm, and 18.5 mm plywood thickness and 150 mm, 100 mm, and 75 mm panel edge nail spacings. It was shown that wood diaphragms could resist capacity design demands for 3-storey structures of all three aspect ratios (1:1, 2:1, 3:1) using the strictest nailing pattern, while demands from the 6 and 9-storey A2 and A3 structures were largely unachievable regardless of plywood thickness and nailing pattern. Based on the results it is recommended that a minimum of moderate ductility (R_D = 3) be required where wooden joisted diaphragms are used in steel frame structures.

It should be noted that drawing conclusions from force demands calculated in computer software alone may be of questionable veracity and the results presented in this research in no way indicative of forces generated in real structures during real seismic events. Force demand values can vary widely based on any number of variations applied to the structural system including SFRS layout, member sizing, and building configuration. The results presented here are meant to capture an overview of what might be reasonably expected using a widely implemented dynamic analysis tool, and certainly do not represent the limits of demand one might see in similar hybrid structures.

An additional observation is made regarding the modeling technique whereby wood diaphragm behaviour is represented by use of linear diagonal braces. While it allows designers to easily create custom stiffness diaphragms, as opposed to shell elements where discretization, boundary constraints and element thickness/type must be considered, the distribution of masses may introduce some error in the model where the mass moment of inertia of the original system is not perfectly replicated which may lead to an inaccurate picture of dynamic response. Additionally, the inclusion of diagonal braces means the lateral load on boundary beams is not captured at all since braces are connected to beam-column nodes exclusively rather than throughout the length of the beam.

CHAPTER 5: **CONCLUSIONS**

5.1 Summary

Design implications of using wood-based flooring systems as an alternative to concrete-steel composite floors in steel frame building structures were assessed based on related research and applicable case studies, current Canadian design code provisions, and finite element modeling. A range of wood-based flooring options including joisted and panel floors were considered and it was shown that structural weight using joisted floors (sawn lumber or engineered joists) can be reduced by roughly 67% compared to the equivalent composite steel-concrete floor, and between 40-60% using timber plank floors, and between 10-50% using CLT floors. Lightest flooring weights are achieved using relatively short (~2.5 m) simply supported spans, rather than longer, continuous spans, though the extra costs incurred from additional fabrication and connection detailing may negate the benefit of the lighter system. A variety of connection detailing options were compared and for the purpose of achieving sufficient in-plane strength for joisted floors a web-fastened wooden ledger providing lateral restraint to the full beam height is considered optimal while bearing panel floors on top flanges rather than bottom flanges provides better lateral restraint, allows for continuous panel spans, and permits development of beam-panel composite behaviour. CLT panels are most eligible for creating composite behaviour where placed over intermediate steel beams due to the higher elastic modulus of layers parallel to the beam; in the event of full composite behaviour being achieved the range of increases in stiffness for 3 – 9-ply CLT is 32-117%, respectively. The issue of determining floor vibrations in wood-steel hybrid floors is a function of floor weight. All wood-based hybrid floors were shown to be much lighter than concrete-steel composite floors indicating the floor vibration estimates based on wood-only floors is preferable to the method used in steel construction. Where deep timber panels with additional concrete topping is used resulting in floor weights similar to steel-concrete floors, the steel design method should be employed.

In-plane deflections of joisted wood-based floors within steel perimeter frames can be estimated through modifications of the existing equation provided in CSA 086. The modification made to the deflection model is based on the designer's assumption regarding the ability of the joist hangers and web-fastened ledger to provide sufficient shear connectivity allowing normal stresses to develop in the steel chords. Regardless, the assumption governs only the flexural and chord splice slip deflection, both of which represent a small portion of the total diaphragm deflection. Results from finite element modeling of 3, 6, and 9-storey concentrically braced frames of 1:1, 2:1, and 3:1 aspect ratios using linear elastic springs to represent in-plane joisted diaphragm stiffness showed that the relative stiffness ratio, r (ratio of diaphragm to frame stiffness), influences the global structural dynamic response for r-values between 0-1. The influence of r on structural response, in terms of base shear and storey deflection, diminishes with increasing storey height as frame stiffness dwarfs the contributions of diaphragm stiffness to overall structural stiffness. Based on CSA 086 allowances the ability of hybrid wood-steel joisted diaphragms to achieve rigid in-plane behaviour ($r \geq 1$) is limited to plan aspect ratios of 1:1, while semi-rigid behaviour can be achieved for aspect ratios of 2:1 and 3:1, though the latter requires 75 mm panel edge nail spacing on 18.5 mm plywood sheathing. Capacity design principles in Clause 9.8 of CSA 086 require non-yielding wood-based diaphragms on non-wood SFRS to resist a total shear force equal to the seismic storey force multiplied by the storey over-strength coefficient. Resulting diaphragm shear demands demonstrated the difficulty in achieving sufficient capacity based on CSA 086 provisions for structures greater than 3-6 storeys in height. Where taller concentrically-braced steel structures using wood joisted floors are desired, it is recommended that a minimum ductility of R_D = 3 be achieved as well as limiting storey over-strength coefficient to a range similar to that used for all-wood structures ($0.9 \leq \gamma \leq 1.2$). In light of the low diaphragm shear capacity it may be in the designer's interest to detail a yielding rather than non-yielding wood diaphragm.

5.2 Future Research

There are many under-investigated topics in timber-steel hybrid structures. Issues relevant to this research which merit further discussion include:

1) Quantifying the influence of perimeter and intermediate steel members on vibration of wood-based joisted floors in steel structures through experimental testing. Parameters to vary could include timber-steel connector type and spacing, joist spacing, concrete topping, blocking, as well as sheathing connectors and spacing.
2) Experimental testing on the composite stiffness and damping properties of CLT panel – steel beam configurations varying panel thickness and connector type and spacing, and concrete topping.
3) Physical experimentation on the ability of web-fastened wooden ledgers to provide sufficient shear transfer to develop axial stresses in steel chords is required to fully understand the in-plane behaviour of wood-based joisted floors in steel structures.
4) Experimental testing on the impact of concrete floor topping and gypsum wall board ceilings on shear capacity of wood-based joisted diaphragms.
5) Non-linear analysis of steel frame structures with yielding wood-based diaphragms to assess energy dissipation and ductility requirements.
6) Non-linear analysis of wood-based diaphragms assessing the benefit of using diagonal springs as opposed to shell elements to represent diaphragm behaviour.

Bibliography

Ashtari, S. (2009). *In-plane Stiffness of Cross-laminated Timber Floors, Master's Thesis.* Vancouver: University of British Columbia.

Blass, H. J., & Fellmoser, P. (2004). Design of solid wood panels with cross layers. *Proceedings of the 8th World Conference on Timber Engineering*, (pp. 2:543-548). Lahti, Finland.

Bott, J. W. (2005). *Horizontal Stiffness of Wood Diaphragms, Master's Thesis.* Blacksburg: Virginia Polytechnic Institute and State University.

Canadian Wood Council. (2010). *Wood Design Manual 2010.* Ottawa: Canadian Standards Association.

CISC. (2006). *Handbook of Steel Construction 9th Edition.* Ottawa: Canadian Standards Association.

Filiatrault, A., Fischer, D., Folz, B., & Uang, C.-M. (2002). Experimental parametric study on the in-plane stiffness of wood diaphragms. *Canadian Journal of Civil Engineering*, 554-566.

FPInnovations. (2011). *CLT Handbook.* Vancouver: FPInnovations.

Green, D. W., Winandy, J. E., & Kretschmann, D. E. (1999). Mechanical Properties of Wood. In *Wood handbook - Wood as an engineering material* (p. 463). Madison: U.S. Department of Agriculture, Forest Service, Forest Products Laboratory.

Hu, L. J., & Gagnon, S. (2010). *Construction Solutions for Wood-Based Floors in Hybrid Building Systems.* Quebec: FPInnovations.

Hu, L., & Gagnon, S. (2012). Controlling Cross-Laminated Timber (CLT) Floor Vibrations: Fundamentals and Method. *World Conference on Timber Engineering.* Auckland.

Huang, X. (2013). *Diaphragm Stiffness in Wood-Frame Construction, Master's Thesis.* Vancouver: University of British Columbia.

ICBO. (1997). *Uniform Building Code.* Whittier, California: International Conference of Building Officials.

Lam, F., & al., e. (2013). Experimental Investigation on Lateral Performance of Timber-Steel Hybrid Shear Wall Systems. *Journal of Structural Engineering*.

Li, S., He, M., Guo, S., & Ni, C. (2010). Lateral Load-Beariing Capacity of Wood Diaphragm in Hybrid Structure with Concrete Frame and Timber Floor. *World Conference on Timber Engineering.* Trentino: WCTE.

Ma, Z., & He, M. (2012). Experimental Analysis of Timber Diaphragm's Capacity on Transferring Horizontal Loads In Timber-Steel Hybrid Structure. *World Conference on Timber Engineering.* Auckland: WCTE.

Metten, A. (2011). *Structural Steel for Canadian Buildings: A Designer's Guide.* Vancouver: Andy Metten.

Moore, M. (2000). Scotia Place - 12 Story Apartment Building: A Case Study of High-Rise Construction Using Wood and Steel - WCTE2000. *NZ Timber Design Journal*, 5-12.

Murray, T. M., Allen, D. E., & Ungar, E. E. (2003). *Floor Vibrations Due to Human Activity.* Chicago: American Institute of Steel Construction, Inc.

Nolan, J., Murray, T. M., Johnson, J. R., Runte, D., & Shue, B. C. (1999). Preventing Annoying Wood Floor Vibrations. *Journal of Structural Engineering*, Vol. 125 No.1 pp.19-24.

Nordic Wood Structures. (2014). *Nordic X-Lam Properties.* Montreal: Nordic Engineered Wood.

StructurLam. (2012). *Cross Laminated Timber Design Guide-Version 7.* Vancouver, BC.

Weyerhaeuser. (2010). *TJI Joist Specifier's Guide (W. Canada).* Federal Way, WA.

Appendix

A.1 Composite Behaviour - Sample

Steel-Timber Composite Beam

CLT Properties

$E_0 := 10000\ MPa$

$E_{90} := \frac{E_0}{30} = 333.333\ MPa$

$f_{b0} := 26.1\ MPa$

$f_{c0} := 11.5\ MPa$

$b_{eff} := 750\ mm$

Steel Properties

$E := 200000\ MPa$

$f_y := 400\ MPa$

$S_x := 1249698\ mm^3$

$I_s := 1.65 \cdot 10^8\ mm^4$

Full Composite Behaviour

3-ply

$a_3 := 102\ mm$

$a_1 := 32\ mm$

$y_{CLT} := 212.6\ mm$

$y_{steel} := 153.3\ mm$

$I_x := 2.17 \cdot 10^8\ mm^4$

$$k_1 := 1 - \left(1 - \frac{E_{90}}{E_0}\right) \cdot \frac{a_1^{\ 3}}{a_3^{\ 3}} = 0.97$$

$$k_2 := \frac{E_{90}}{E_0} + \left(1 - \frac{E_{90}}{E_0}\right) \cdot \frac{a_1^{\ 3}}{a_3^{\ 3}} = 0.063$$

$$k_3 := 1 - \left(1 - \frac{E_{90}}{E_0}\right) \cdot \frac{a_1}{a_3} = 0.697$$

$$k_4 := \frac{E_{90}}{E_0} + \left(1 - \frac{E_{90}}{E_0}\right) \cdot \frac{a_1}{a_3} = 0.337$$

Effective Values

$f_{c90eff} := f_{c0} \cdot k_4 = 3.871\ \boldsymbol{MPa}$

$E_{c90eff} := E_0 \cdot k_4 = \left(3.366 \cdot 10^{3}\right)\ \boldsymbol{MPa}$

$f_{b90eff} := f_{b0} \cdot k_2 \cdot \dfrac{a_3}{a_1} = 5.256\ \boldsymbol{MPa}$

$E_{b90eff} := E_0 \cdot k_2 = 631.821\ \boldsymbol{MPa}$

Bending Strength & Stiffness - Composite

$M_r := f_{c90eff} \cdot \left(\dfrac{E}{E_{c90eff}}\right) \cdot \left(\dfrac{I_x}{y_{CLT}}\right) = 234.76\ \boldsymbol{kN \cdot m}$

$\dfrac{M_r}{S_x \cdot f_y} = 0.47$

$EI_{comp} := E \cdot I_x = \left(4.34 \cdot 10^{13}\right)\ \boldsymbol{N \cdot mm^2}$

$C_3 := \dfrac{EI_{comp}}{EI_{steel}} = 1.315$

Bending Strength & Stiffness - Sum

$EI_{CLT} := E_{b90eff} \cdot b_{eff} \cdot \dfrac{{a_3}^{3}}{12} = \left(4.191 \cdot 10^{10}\right)\ \boldsymbol{N \cdot mm^2}$

$EI_{steel} := E \cdot I_s = \left(3.3 \cdot 10^{13}\right)\ \boldsymbol{N \cdot mm^2}$

$S_3 := \dfrac{\left(EI_{CLT} + EI_{steel}\right)}{EI_{steel}} = 1.001$

A.2 Structural Weight – Sample (Glulam)

Loading & Dimensions

$q_f := 7.225\ kPa$ $\quad q_{LL} := 1.9\ kPa$ Floor Load

$l_{bay} := 7.5\ m$

$l_c := l_{bay} - 2 \cdot \frac{150\ mm}{2} = 7350\ mm$ Bay length - beam bearing length = clear span

$w_f := q_f \cdot 1\ m = 7.2\ \frac{kN}{m}$ Load per metre width

$w_{LL} := q_{LL} \cdot 1\ m = 1.9\ \frac{kN}{m}$ Live Load per metre width

Single Span	Two Span	Three Span
$M_{f1} := \frac{w_f \cdot l_c^2}{8} = 48.8\ kN \cdot m$	$M_{f2} := \frac{w_f \cdot l_c^2}{8} = 48.8\ kN \cdot m$	$M_{f3} := \frac{w_f \cdot l_c^2}{10} = 39\ kN \cdot m$
$V_{f1} := \frac{(w_f \cdot l_c)}{2} = 26.6\ kN$	$V_{f2} := 1.25 \cdot w_f \cdot l_c = 66.4\ kN$	$V_{f3} := 1.10\ w_f \cdot l_c = 58.4\ kN$

$\Delta_{allowable} := \frac{l_c}{360} = 20.417\ mm$

086 Clause 6.5.2 Orientation - If glulams are oriented as planks design as if they are built-up beams with sawn lumber members of No.2 Grade.
So recheck the previous calculations using available glulam sizes to optimize.

$b_{GL} := 494\ mm$ $\quad h_{GL} := 135\ mm$ $\quad n := 2$

Kz
89mm - 1.7
140mm - 1.4
191mm - 1.2
235mm - 1.1
286mm - 1.0

Moment

$\phi := 0.9$

$f_b := 11.8\ MPa$ Subject to change

$K_D := 1.0$ $\quad K_H := 1.1$ $\quad K_{Sb} := 1.0$ $\quad K_T := 1.0$ $\quad K_{Zb} := 1.4$ $\quad K_L := 1.0$

$F_b := f_b \cdot (K_D \cdot K_H \cdot K_{Sb} \cdot K_T) = 12.98\ MPa$

$S := \frac{\left(b_{GL} \cdot h_{GL}^2\right)}{6} = \left(1.501 \cdot 10^6\right)\ mm^3$

$M_r := \phi \cdot F_b \cdot S \cdot K_{Zb} \cdot K_L = 24.541\ kN \cdot m$ 086 Cl. 5.5.4

$M_{rGL} := M_r \cdot n = 49.082\ kN \cdot m$ Resistance per metre

1 span	2 span	3 span
$\frac{M_{rGL}}{M_{f1}} = 1.006$	$\frac{M_{rGL}}{M_{f3}} = 1.257$	$\frac{M_{rGL}}{M_{f3}} = 1.257$

Shear

$f_v := 1.5\ \mathbf{MPa} \qquad K_{Sv} := 1.1 \quad K_{Zv} := K_{Zb}$

$A_n := b_{GL} \cdot h_{GL} = \left(6.669 \cdot 10^{4}\right)\ \mathbf{mm}^{2}$

$F_v := f_v \cdot K_D \cdot K_H \cdot K_{Sv} \cdot K_T$

$V_r := \phi \cdot F_v \cdot \frac{2\ A_n}{3} \cdot K_{Zv} = 101.676\ \mathbf{kN}$ *086 Cl. 5.5.5*

$V_{rGL} := V_r \cdot n = 203.351\ \mathbf{kN}$ *Resistance per metre*

1 span	2 span	3 span
$\frac{V_{rGL}}{V_{f1}} = 7.659$	$\frac{V_{rGL}}{V_{f2}} = 3.063$	$\frac{V_{rGL}}{V_{f3}} = 3.481$

Deflection

$E := 9500\ \mathbf{MPa} \qquad K_{SE} := 1.0$
$E_S := E \cdot K_{SE} \cdot K_T$

$I := \frac{\left(b_{GL} \cdot h_{GL}^{3}\right)}{12} \cdot n = \left(2.026 \cdot 10^{8}\right)\ \mathbf{mm}^{4}$

1 span	2 span	3 span
$\frac{\Delta_{allowable}}{\left(\frac{5 \cdot w_{LL} \cdot l_c^{4}}{384\ E_S \cdot I}\right)} = 0.544$	$\frac{\Delta_{allowable}}{\left(\frac{w_{LL} \cdot l_c^{4}}{185\ E_S \cdot I}\right)} = 1.311$	$\frac{\Delta_{allowable}}{\left(0.0069 \cdot \frac{w_{LL} \cdot l_c^{4}}{E_S \cdot I}\right)} = 1.027$

Weight *per sq.metre of flooring*

$W_{GL} := 440\ \frac{\mathbf{kg}}{\mathbf{m}^{3}} \cdot h_{GL} = 59.4\ \frac{\mathbf{kg}}{\mathbf{m}^{2}}$ *Density from 086 Table A.10.1*

A.3 Code Diaphragm Deflection – Sample

Width	10000	mm
q	0.00258	N/mm^2
Bv	8500	N/mm
Es	200000	MPa
As	12900	mm^2
Rd	3	
Ro	1.3	

Load Per Nail (N)	Deformation (mm)
0	0.12
100	0.12
200	0.12
300	0.12
400	0.18
500	0.25
600	0.33
700	0.43
800	0.57
900	0.74
1000	0.98

Nail Spacing (mm)	# of nails	Load per nail (N)	Nail Deformation (mm)	Nail Slip Deflection (mm)	Shear Deflection (mm)
150	67	1838	0.98	6.02	5.57
100	100	1226	0.98	6.02	5.57
75	133	919	0.74	4.54	5.57
150	67	1838	0.98	6.02	4.44
100	100	1226	0.98	6.02	4.44
75	133	919	0.74	4.54	4.44
150	67	1838	0.98	6.02	3.65
100	100	1226	0.98	6.02	3.65
75	133	919	0.74	4.54	3.65
150	67	1838	0.98	6.02	3.13
100	100	1226	0.98	6.02	3.13
75	133	919	0.74	4.54	3.13

Flexural Deflection (mm)	Total Deflection (mm)	Global Stiffness (N/mm)	r	Name	Shear Strength (kN)
0.02	11.61	21106.76	0.75	P9.5-N150-H3-A1	68.6
0.02	11.61	21106.76	0.75	P9.5-N100-H3-A1	102.9
0.02	10.14	24174.47	1.00	P9.5-N75-H3-A1	116.2
0.02	10.48	23382.59	1.00	P12.5-N150-H3-A1	81.9
0.02	10.48	23382.59	1.00	P12.5-N100-H3-A1	123.9
0.02	9.01	27207.47	1.00	P12.5-N75-H3-A1	140.0
0.02	9.69	25296.05	1.00	P15.5-N150-H3-A1	91.0
0.02	9.69	25296.05	1.00	P15.5-N100-H3-A1	137.2
0.02	8.22	29833.27	1.25	P15.5-N75-H3-A1	156.1
0.02	9.17	26733.67	1.00	P18.5-N150-H3-A1	91.0
0.02	9.17	26733.67	1.00	P18.5-N100-H3-A1	137.2
0.02	7.69	31853.45	1.25	P18.5-N75-H3-A1	156.1